Med Chem Res (2016) 25:1096–1114
DOI 10.1007/s00044-016-1528-8

MEDICINAL CHEMISTRY RESEARCH

ORIGINAL RESEARCH

Convenient synthesis, anticancer evaluation and QSAR studies of some thiazole tethered indenopyrazoles

Satbir Mor[1] · Savita Nagoria[1] · Ashwani Kumar[2] · Jitender Monga[3] · Sandeep Lohan[4]

Received: 6 November 2015 / Accepted: 4 February 2016 / Published online: 16 March 2016

Abstract A convenient one-pot synthesis of twelve new thiazole tethered indeno[1,2-*c*]pyrazol-4-ones (**3a–3l**) was carried out by three-component reaction between 1,3-diketones, thiosemicarbazide and α-bromoketones in high yields. Wolff-Kishner reduction of indeno[1,2-*c*]pyrazol-4-ones (**3a–3l**) led to the formation of corresponding indeno[1,2-*c*]pyrazoles (**4a–4l**) in moderate-to-good yields. The structures of all the synthesized indenopyrazoles were elucidated by IR, ^{1}H NMR, ^{13}C NMR and mass spectral techniques. In vitro cytotoxicity of thiazole tethered indenopyrazoles (**3a–3l** & **4a–4l**) was evaluated against different human cancer cell lines, viz. human renal carcinoma (A498), human colorectal adenocarcinoma (HT29), human breast adenocarcinoma (MCF-7), human hepatocellular carcinoma (HepG2) and normal cell line, i.e., normal rat kidney epithelial (NRK). Among all the tested derivatives, **4a**, **4d** and **4h** exhibited better activity against HT29 cancer cell line. The statistically significant QSAR models were developed for all the cancer cell lines using multiple linear regression analysis to understand the observed activity trend on structural basis.

Graphical Abstract

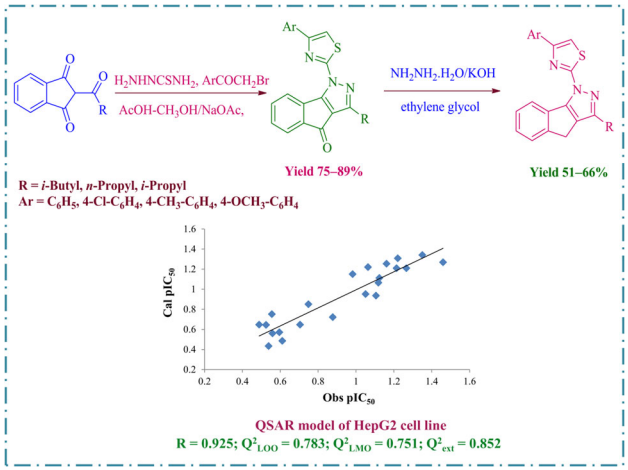

Keywords One-pot synthesis · Three-component reaction · Indenopyrazoles · Anticancer · QSAR

Introduction

Cancer remains one of the most difficult life-threatening diseases to treat, although a lot of progress has been made in chemotherapy research in recent years. Therefore, the discovery of more efficacious and safer anticancer therapeutic agents is one of the fundamental goals in medicinal chemistry research. The pharmacoactive agents containing

Electronic supplementary material The online version of this article (doi:10.1007/s00044-016-1528-8) contains supplementary material, which is available to authorized users.

✉ Satbir Mor
satbir_mor@yahoo.co.in

[1] Department of Chemistry, Guru Jambheshwar University of Science & Technology, Hisar, Haryana 125001, India

[2] Department of Pharmaceutical Sciences, Guru Jambheshwar University of Science & Technology, Hisar, Haryana 125001, India

[3] Department of Urology, Postgraduate Institute of Medical Education and Research, Chandigarh 160012, India

[4] Department of Pharmacy, Jaypee University of Information Technology, Solan, Himachal Pradesh 173234, India

pyrazole scaffolds have received considerable attention owing to their anticancer activities (Abdou *et al.*, 2004; Deverakonda *et al.,* 2013; Maggio *et al.*, 2014). Pyrazole motif makes up the core structure of numerous biologically active compounds (Elguero *et al.*, 2002) including blockbuster drugs such as Celebrex (Penning *et al.*, 1997) and Viagra (Terrett *et al.*, 1996). Among the pyrazoles, particularly the indenopyrazoles have received extensive awareness in recent years due to their synthetic significance and broad range of biological activities (Lapenna and Giordano, 2009; Mohil *et al.*, 2014; Usui *et al.*, 2008; Yue *et al.*, 2004). For instance, indeno[1,2-*c*]pyrazole-2-carboxamide/carbothioamide have recently been recognized as novel antitubercular analogues (Ahsan *et al.*, 2011) and indeno[1,2-*c*]pyrazol-4-ones as potent and selective cyclin-dependent kinase (CDK) (Nugiel *et al.*, 2002) and check point kinase (CHK1) inhibitors (Tao *et al.,* 2005, 2007) showing admirable activity against various tumor cell linings. Indeno[1,2-*c*]pyrazoles are also known to act as potential CNS agents (Lemke *et al.*, 1978), tyrosine kinase inhibitors (Yan *et al.*, 2006), antidepressants (Flores and Loev, 1961; Loev and Mosher, 1961) and nonsteroidal anti-inflammatory drugs (Lemke *et al.*, 1989). Consequently, various approaches have been developed for the synthesis of indenopyrazoles (Hamilton, 1976; Lemke and Sawhney, 1982; Minegishi *et al.,* 2013; Mosher and Soeder, 1971; Usui *et al.,* 2008). Similarly, thiazole derivatives also constitute a fascinating class of organic compounds as they have been endowed with ample number of pharmacological activities like anticancer (Gu and Jin, 2012; Kim *et al.,* 2002; Misra *et al.,* 2004), anticonvulsant (Arshad *et al.*, 2014), analgesic (Thore *et al.,* 2013), antimicrobial (Gaikwad *et al.*, 2013), anti-inflammatory (Bhosale *et al.,* 2012), antipyretic (Pignatello *et al.,* 1991), antitubercular (Samadhiya *et al.,* 2013), anti-HIV (Rawal *et al.,* 2008), antioxidant (Shih *et al.,* 2007), diuretic (Andreani *et al.,* 1987), anti-allergic (Hargrave *et al.,* 1983), antihypertensive (Patt *et al.,* 1992), etc.

The precedent for broad bioactivity profiles for indenopyrazole and thiazole pharmacophores led us to perceive that fusion of these motifs might result in new bioactive molecules with interesting biological activities. For instance, thiazole-linked pyrazoles are endowed with anticancer (Altıntop *et al.,* 2014; Chong and Duvadie, 2003; Dawood *et al.,* 2013; Wang *et al.,* 2013), anti-inflammatory (Bekhit *et al.,* 2008; Farghaly *et al.,* 2000), antimicrobial (Bekhit *et al.,* 2008; Farghaly *et al.,* 2000; Gaikwad *et al.,* 2013; Mor *et al.,* 2012a; Karale *et al.,* 2015; Song *et al.,* 2014) activities, etc. In addition, thiazole tethered indenopyrazoles have been recognized as cyclin-dependent kinase (CDK) inhibitors (Rostom, 2006; Yue *et al.*, 2004). The above facts prompted us to direct our study toward the synthesis of new structural entities combining the indenopyrazole and thiazole scaffolds together in a molecular framework with a goal to explore their anticancer activity.

Further, Quantitative Structure Activity Relationship (QSAR) is a thriving technique that has gained considerable attention during the past decades because of good success in medicinal chemistry research, proteomics, metabolomics and bioinformatics (Tong *et al.,* 2014). QSAR is a multivariate, mathematical relationship between a set of physicochemical properties and biological activity (Suresh, 2013) and has been successfully employed for drug design and prediction of drug activity (Sigroha *et al.,* 2012).

In this perspective and in a quest for synthesizing biologically active nitrogen and sulfur heterocycles (Mor *et al.,* 2012a, b, c), herein, we report a convenient synthesis, in vitro anticancer evaluation and QSAR studies of twenty-four new thiazole tethered indenopyrazoles (**3a–3l** & **4a–4l**).

Materials and methods

Chemistry

All reagents were used as received from commercial suppliers without any additional purification. Melting points (mp, °C) of the synthesized compounds were determined in open capillaries on an Electrothermal Melting Point apparatus, LABCO Co, India, and are uncorrected. The FTIR spectra were recorded in KBr on IR affinity-1 FTIR (Shimadzu) spectrophotometer, and wave numbers (ν) are reported in cm^{-1}. ^{1}H NMR, ^{13}C NMR, DEPT (distortionless enhancement by polarization transfer), and 2D-NMR [COSY (correlation spectroscopy), HSQC (heteronuclear single-quantum coherence) and HMBC (heteronuclear multiple bond correlation)] spectra were scanned on Bruker AVANCE II NMR spectrometer operating at 300/400 MHz using tetramethylsilane (TMS) as internal standard. Chemical shift (δ) values are given in parts per million (ppm), and coupling constants (J) are expressed in Hertz (Hz). Mass spectra were recorded on Waters Quadrupole Detector (TDQ) by electron spray ionization (ESI) technique in positive mode. Elemental analyses were performed on Thermo Scientific FLASH-2000 CHN analyser. Analytical results for C, H and N were found to be within ±0.4 % of the theoretical values. The purity of synthesized compounds was tested using precoated TLC plates (SIL G/UV_{554}, ALUGRAM), and visualization was achieved via UV light.

General procedure for the synthesis of indeno[1,2-c]pyrazol-4(1H)-ones (**3**) The 2-acyl-(1*H*)-indene-

1,3(2*H*)-diones (**1**) needed for the purpose were prepared by the Claisen condensation of diethylphthlate and appropriate ketone under the influence of sodium methoxide according to the procedure as described in literature (Dhawan *et al.,* 1993; Shapiro *et al.,* 1960). An equimolar mixture of 2-acyl-(1*H*)-indene-1,3(2*H*)-diones (**1**, 5 mmol) and thiosemicarbazide (5 mmol) in dry methanol (30 mL) was refluxed on water bath at 65 °C for 10–15 min. Thereafter, appropriate phenacyl bromide (**2**, 5 mmol), sodium acetate (0.41 g, 5 mmol) and glacial acetic acid (15 mL) were added to the above solution, and the reaction mixture was refluxed on a water bath at 80–85 °C for 6–7 h. Thereafter, the reaction mixture was concentrated and the solid thus obtained was separated by filtration and recrystallized from chloroform to furnish the target thiazole tethered indeno[1,2-*c*]pyrazol-4(1*H*)-ones (**3a**–**3l**) in high yields. The physical and spectral data of **3a**–**3l** are described as follows:

*3-Isobutyl-1-(4-phenylthiazol-2-yl)indeno[1,2-c]pyrazol-4(1H)-one (**3a**)* Yellowish green crystals; yield 81 %; mp 172–176 °C; IR (KBr): ν_{max} 741, 1080, 1383, 1487, 1528, 1597 (C = N), 1703 (C = O), 2882, 2949 (aliphatic C–H stretch), 3078, 3111 (aromatic C–H stretch) cm^{-1}; ^1H NMR (300 MHz, $CDCl_3$): $\delta = 1.02$ (d, 6H, $J = 6.6$ Hz, $–CH_2CH(C\underline{H_3})_2$), 2.25–2.34 (m, 1H, $–CH_2C\underline{H}(CH_3)_2$), 2.65 (d, 2H, $J = 7.20$ Hz, $–C\underline{H_2}CH(CH_3)_2$), 7.32–7.53 (m, 6H, H-6, H-7, H-5′, H-3″, H-4″, H-5″), 7.59 (d, 1H, $J = 7.20$ Hz, H-5), 7.93 (d, 2H, $J = 8.40$ Hz, H-2″, H-6″), 8.48 (d, 1H, $J = 7.50$ Hz, H-8); ^{13}C NMR (100 MHz, $CDCl_3$): $\delta = 22.46$ ($–CH_2CH(\underline{CH_3})_2$), 27.83 ($–CH_2\underline{CH}(CH_3)_2$), 36.31 ($–\underline{CH_2}CH(CH_3)_2$), 110.75 (C-5′), 123.41 (C-3a), 123.84 (C-8), 124.22 (C-5), 126.10 (C-3″, C-5″), 128.57 (C-4″), 128.98 (C-2″, C-6″), 130.48 (C-6), 132.78 (C-1″), 133.42 (C-7), 134.05 (C-4a), 140.26 (C-8a), 152.42 (C-3), 153.22 (C-4′), 157.72 (C-8b), 160.03 (C-2′), 184.00 (C-4); ESI–MS *m/z*: 386.1 $[M + 1]^+$; Anal. Calcd. for $C_{23}H_{19}N_3OS$ (385.12): C, 71.66; H, 4.97; N, 10.90. Found: C, 71.85; H, 5.17; N, 10.69.

*1-(4-(4-Chlorophenyl)thiazol-2-yl)-3-isobutylindeno[1,2-c]pyrazol-4(1H)-one (**3b**)* Green crystals; yield 89 %; mp 184–189 °C; IR (KBr): ν_{max} 742, 1092, 1387, 1481, 1528, 1597 (C = N), 1707 (C = O), 2872, 2957 (aliphatic C–H stretch), 3063, 3100 (aromatic C–H stretch) cm^{-1}; ^1H NMR (300 MHz, $CDCl_3$): $\delta = 1.01$ (d, 6H, $J = 6.60$ Hz, $–CH_2CH(C\underline{H_3})_2$), 2.24–2.34 (m, 1H, $–CH_2C\underline{H}(CH_3)_2$), 2.64 (d, 2H, $J = 7.50$ Hz, $–C\underline{H_2}CH(CH_3)_2$), 7.31–7.49 (m, 5H, H-6, H-7, H-5′, H-3″, H-5″), 7.59 (d, 1H, $J = 7.20$ Hz, H-5), 7.84 (d, 2H, $J = 8.40$ Hz, H-2″, H-6″), 8.39 (d, 1H, $J = 7.50$ Hz, H-8); ^{13}C NMR (100 MHz, $CDCl_3$): $\delta = 22.47$ ($–CH_2CH(\underline{CH_3})_2$), 27.83 ($–CH_2\underline{CH}(CH_3)_2$), 36.31 ($–\underline{CH_2}CH(CH_3)_2$), 111.01 (C-5′), 123.53 (C-3a), 123.63 (C-8), 124.30 (C-5), 127.32 (C-2″, C-6″), 129.17 (C-3″, C-5″), 130.54 (C-6), 132.52 (C-1″), 132.72 (C-4″), 133.31 (C-7), 134.42 (C-4a), 140.25 (C-8a), 152.06 (C-3), 152.54 (C-4′), 157.71 (C-8b), 160.29 (C-2′), 183.90 (C-4); ESI–MS *m/z*: 419.1 $[M]^+$, 420.3 $[M + 1]^+$; Anal. Calcd. for $C_{23}H_{18}ClN_3OS$ (419.09): C, 65.78; H, 4.32; N, 10.01. Found: C, 65.42; H, 4.58; N, 9.88.

*3-Isobutyl-1-(4-p-tolylthiazol-2-yl)indeno[1,2-c]pyrazol-4(1H)-one (**3c**)* Greenish yellow crystals; yield 87 %; mp 158–164 °C; IR (KBr): ν_{max} 741, 1086, 1385, 1493, 1529, 1601 (C = N), 1713 (C = O), 2949 (aliphatic C–H stretch), 3111 (aromatic C–H stretch) cm^{-1}; ^1H NMR (400 MHz, $CDCl_3$): $\delta = 1.01$ (d, 6H, $J = 6.64$ Hz, $–CH_2CH(C\underline{H_3})_2$), 2.23–2.34 (m, 1H, $–CH_2C\underline{H}(CH_3)_2$), 2.42 (s, 3H, $C\underline{H_3}$), 2.63 (d, 2H, $J = 7.32$ Hz, $–C\underline{H_2}CH(CH_3)_2$), 7.23–7.47 (m, 5H, H-6, H-7, H-5′, H-3″, H-5″), 7.57 (d, 1H, $J = 7.20$ Hz, H-5), 7.79 (d, 2H, $J = 7.96$ Hz, H-2″, H-6″), 8.44 (d, 1H, $J = 7.36$ Hz, H-8); ^{13}C NMR (100 MHz, $CDCl_3$): $\delta = 21.35$ ($\underline{CH_3}$), 22.50 ($–CH_2$-$CH(\underline{CH_3})_2$), 27.88 ($–CH_2\underline{CH}(CH_3)_2$), 36.36 ($–\underline{CH_2}$-$CH(CH_3)_2$), 109.92 (C-5′), 123.42 (C-3a), 123.90 (C-8), 124.25 (C-5), 126.05 (C-3″, C-5″), 129.68 (C-2″, C-6″), 130.47 (C-6), 131.41 (C-1″), 132.86 (C-4a), 133.40 (C-7), 138.57 (C-4″), 140.34 (C-8a), 152.46 (C-3), 153.35 (C-4′), 157.75 (C-8b), 159.94 (C-2′), 184.08 (C-4); ESI–MS *m/z*: 400.43 $[M + 1]^+$; Anal. Calcd. for $C_{24}H_{21}N_3OS$ (399.14): C, 72.15; H, 5.30; N, 10.52. Found: C, 72.36; H, 5.07; N, 10.78.

*3-Isobutyl-1-(4-(4-methoxyphenyl)thiazol-2-yl)indeno[1,2-c]pyrazol-4(1H)-one (**3d**)* Green crystals; yield 88 %; mp 180–190 °C; IR (KBr): ν_{max} 737, 1090, 1387, 1489, 1529, 1601 (C = N), 1707 (C = O), 2887, 2949 (aliphatic C–H stretch), 3019, 3096 (aromatic C–H stretch) cm^{-1}; ^1H NMR (400 MHz, $CDCl_3$): $\delta = 1.03$ (d, 6H, $J = 6.60$ Hz, $–CH_2CH(C\underline{H_3})_2$), 2.28–2.35 (m, 1H, $–CH_2C\underline{H}(CH_3)_2$), 2.66 (d, 2H, $J = 7.32$ Hz, $–C\underline{H_2}CH(CH_3)_2$), 3.91 (s, 3H, $OC\underline{H_3}$), 7.04 (2H, d, $J = 8.72$ Hz, H-3″, H-5″), 7.21 (s, 1H, H-5′), 7.34–7.51 (m, 2H, H-6, H-7), 7.60 (d, 1H, $J = 7.16$ Hz, H-5), 7.85 (d, 2H, $J = 8.72$ Hz, H-2″, H-6″), 8.46 (d, 1H, $J = 7.40$ Hz, H-8); ^{13}C NMR (100 MHz, $CDCl_3$): $\delta = 22.49$ ($–CH_2CH(\underline{CH_3})_2$), 27.87 ($–CH_2\underline{CH}(CH_3)_2$), 36.35($–\underline{CH_2}CH(CH_3)_2$), 55.42 ($O\underline{CH_3}$), 108.91 (C-5′), 114.34 (C-3″, C-5″), 123.40 (C-3a), 123.84 (C-8), 124.26 (C-5), 127.00 (C-1″), 127.44 (C-2″, C-6″), 130.46 (C-6), 132.86 (C-4a), 133.38 (C-7), 140.34 (C-8a), 152.46 (C-3), 153.08 (C-4′), 157.70 (C-8b), 159.93 (2C, C-2′ & C-4″), 184.07 (C-4); ESI–MS *m/z*: 416.1 $[M + 1]^+$, 417.2 $[M + 2]^+$, 438.6 $[M + Na]^+$; Anal. Calcd. for $C_{24}H_{21}N_3$-O_2S (415.14): C, 69.37; H, 5.09; N, 10.11. Found: C, 69.52; H, 5.37; N, 10.42.

*1-(4-Phenylthiazol-2-yl)-3-propylindeno[1,2-c]pyrazol-4(1H)-one (**3e**)* Yellow solid; yield 80 %; mp

120–124 °C; IR (KBr): ν_{max} 739, 1088, 1474, 1535, 1605 (C = N), 1705 (C = O), 2853, 2959 (aliphatic C–H stretch), 3061, 3134 (aromatic C–H stretch) cm^{-1}; ^1H NMR (400 MHz, $CDCl_3$): δ = 1.03 (t, 3H, –$CH_2CH_2C\underline{H_3}$), 1.85–1.90 (m, 2H, –$CH_2C\underline{H_2}CH_3$), 2.73 (t, 2H, –$\underline{CH_2}CH_2CH_3$), 7.32–7.51 (m, 6H, H-6, H-7, H-5′, H-3″, H-4″, H-5″), 7.58 (d, 1H, *J* = 7.16 Hz, H-5), 7.91 (d, 2H, *J* = 8.40 Hz, H-2″, H-6″), 8.45 (d, 1H, *J* = 7.40 Hz, H-8); ^{13}C NMR (100 MHz, $CDCl_3$): δ = 13.90 (–$CH_2CH_2\underline{CH_3}$), 21.44 (–$CH_2\underline{CH_2}CH_3$), 29.50 (–$\underline{CH_2}CH_2CH_3$), 110.70 (C-5′), 123.22 (C-3a), 123.89 (C-8), 124.29 (C-5), 126.15 (C-3″, C-5″), 128.61 (C-4″), 129.01 (C-2″, C-6″), 130.52 (C-6), 132.85 (C-1″), 133.43 (C-7), 134.09 (C-4a), 140.30 (C-8a), 153.23 (C-3), 153.28 (C-4′), 157.88 (C-8b), 160.07 (C-2′), 184.04 (C-4); ESI–MS *m/z*: 372.58 $[M + 1]^+$; Anal. Calcd. for $C_{22}H_{17}N_3OS$ (371.11): C, 71.14; H, 4.61; N, 11.31. Found: C, 71.38; H, 4.92; N, 11.63.

1-(4-(4-Chlorophenyl)thiazol-2-yl)-3-propylindeno[1,2-c]pyrazol-4(1H)-one (***3f***) Green crystals; yield 83 %; mp 185–188 °C; IR (KBr): ν_{max} 746, 1094, 1474, 1541, 1603 (C = N), 1701 (C = O), 2849, 2957 (aliphatic C–H stretch), 3090 (aromatic C–H stretch) cm^{-1}; ^1H NMR (400 MHz, $CDCl_3$): δ = 1.03 (t, 3H, –$CH_2CH_2C\underline{H_3}$), 1.80–1.91 (m, 2H, –$CH_2C\underline{H_2}CH_3$), 2.72 (t, 2H, –$\underline{CH_2}CH_2CH_3$), 7.25–7.45 (5H, m, H-6, H-7, H-5′, H-3″, H-5″), 7.57 (d, 1H, *J* = 7.12 Hz, H-5), 7.81 (d, 2H, *J* = 8.36 Hz, H-2″, H-6″), 8.35 (d, 1H, *J* = 7.36 Hz, H-8); ^{13}C NMR (100 MHz, $CDCl_3$): δ = 13.86 (–$CH_2CH_2\underline{CH_3}$), 21.38 (–$CH_2\underline{CH_2}CH_3$), 29.48 (–$\underline{CH_2}CH_2CH_3$), 111.00 (C-5′), 123.33 (C-3a), 123.65 (C-8), 124.32 (C-5), 127.35 (C-2″, C-6″), 129.19 (C-3″, C-5″), 130.56 (C-6), 132.57 (C-1″), 132.78 (C-4″), 133.32 (C-7), 134.47 (C-4a), 140.28 (C-8a), 152.12 (C-3), 153.29 (C-4′), 157.85 (C-8b), 160.32 (C-2′), 183.86 (C-4); ESI–MS *m/z*: 406.66 $[M + 1]^+$, 407.68 $[M + 2]^+$, 408.72 $[M + 3]^+$; Anal. Calcd. for $C_{22}H_{16}ClN_3OS$ (405.07): C, 65.10; H, 3.97; N, 10.35. Found: C, 65.37; H, 4.23; N, 10.62.

3-Propyl-1-(4-p-tolylthiazol-2-yl)indeno[1,2-c]pyrazol-4(1H)-one (***3g***) Yellow solid; yield 84 %; mp 175–177 °C; IR (KBr): ν_{max} 739, 1092, 1474, 1541, 1605 (C = N), 1705 (C = O), 2872, 2963 (aliphatic C–H stretch), 3026, 3119 (aromatic C–H stretch) cm^{-1}; ^1H NMR (400 MHz, $CDCl_3$): δ = 1.03 (t, 3H, –$CH_2CH_2C\underline{H_3}$), 1.82–1.91 (m, 2H, –$CH_2C\underline{H_2}CH_3$), 2.42 (s, 3H, $C\underline{H_3}$), 2.72 (t, 2H, –$\underline{CH_2}CH_2CH_3$), 7.25–7.47 (5H, m, H-6, H-7, H-5′, H-3″, H-5″), 7.57 (d, 1H, *J* = 7.16 Hz, H-5), 7.79 (d, 2H, *J* = 8.08 Hz, H-2″, H-6″), 8.44 (d, 1H, *J* = 7.40 Hz, H-8); ^{13}C NMR (100 MHz, $CDCl_3$): δ = 13.90 (–$CH_2CH_2\underline{CH_3}$), 21.35 ($\underline{CH_3}$), 21.44 (–$CH_2\underline{CH_2}CH_3$), 29.49 (–$\underline{CH_2}CH_2CH_3$), 109.90 (C-5′), 123.15 (C-3a), 123.92 (C-8), 124.24 (C-5), 126.04 (C-3″, C-5″), 129.67 (C-2″, C-6″), 130.48 (C-6), 131.38 (C-1″), 132.85 (C-4a), 133.39 (C-7), 138.56 (C-4″), 140.30 (C-8a), 153.17 (C-3), 153.34 (C-4′), 157.82 (C-8b), 159.89 (C-2′), 184.05 (C-4); ESI–MS *m/z*: 386.70 $[M + 1]^+$, 408.32 $[M + Na]^+$; Anal. Calcd. for $C_{23}H_{19}N_3OS$ (385.12): C, 71.66; H, 4.97; N, 10.90. Found: C, 71.89; H, 4.71; N, 10.68.

1-(4-(4-Methoxyphenyl)thiazol-2-yl)-3-propylindeno[1,2-c]pyrazol-4(1H)-one (***3h***) Yellow solid; yield 81 %; mp 184–186 °C; IR (KBr): ν_{max} 760, 1090, 1475, 1541, 1610 (C = N), 1703 (C = O), 2868, 2961 (aliphatic C–H stretch), 3030, 3115 (aromatic C–H stretch) cm^{-1}; ^1H NMR (400 MHz, $CDCl_3$): δ = 1.03 (t, 3H, –$CH_2CH_2C\underline{H_3}$), 1.83–1.92 (m, 2H, –$CH_2C\underline{H_2}CH_3$), 2.73 (t, 2H, –$\underline{CH_2}CH_2CH_3$), 3.88 (s, 3H, $OC\underline{H_3}$), 7.01 (2H, d, *J* = 8.72 Hz, H-3″, H-5″), 7.18 (s, 1H, H-5′), 7.32–7.48 (m, 2H, H-6, H-7), 7.58 (d, 1H, *J* = 7.16 Hz, H-5), 7.84 (d, 2H, *J* = 8.68 Hz, H-2″, H-6″), 8.44 (d, 1H, *J* = 7.40 Hz, H-8); ^{13}C NMR (100 MHz, $CDCl_3$): δ = 13.90 (–$CH_2CH_2\underline{CH_3}$), 21.44 (–$CH_2\underline{CH_2}CH_3$), 29.50 (–$\underline{CH_2}CH_2CH_3$), 55.42 ($O\underline{CH_3}$), 108.90 (C-5′), 114.35 (C-3″, C-5″), 123.16 (C-3a), 123.86 (C-8), 124.27 (C-5), 127.01 (C-1″), 127.45 (C-2″, C-6″), 130.48 (C-6), 132.89 (C-4a), 133.39 (C-7), 140.34 (C-8a), 153.10 (C-3), 153.19 (C-4′), 157.80 (C-8b), 159.90 (C-2′), 159.94 (C-4″), 184.05 (C-4); ESI–MS *m/z*: 402.73 $[M + 1]^+$; Anal. Calcd. for $C_{23}H_{19}N_3O_2S$ (401.12): C, 68.81; H, 4.77; N, 10.47. Found: C, 68.58; H, 4.93; N, 10.12.

3-Isopropyl-1-(4-phenylthiazol-2-yl)indeno[1,2-c]pyrazol-4(1H)-one (***3i***) Yellow solid; yield 78 %; mp 140–144 °C; IR (KBr): ν_{max} 744, 878, 1094, 1475, 1543, 1605 (C = N), 1703 (C = O), 2880, 2968 (aliphatic C–H stretch), 3069, 3116 (aromatic C–H stretch) cm^{-1}; ^1H NMR (400 MHz, $CDCl_3$): δ = 1.41 (d, 6H, *J* = 6.92 Hz, –$CH(C\underline{H_3})_2$), 3.06–3.13 (m, 1H, –$C\underline{H}(CH_3)_2$), 7.32–7.51 (6H, m, H-6, H-7, H-3″, H-4″, H-5″, H-5′), 7.58 (d, 1H, *J* = 7.24 Hz, H-5), 7.91 (d, 2H, *J* = 8.00 Hz, H-2″, H-6″), 8.46 (d, 1H, *J* = 7.32 Hz, H-8); ^{13}C NMR (100 MHz, $CDCl_3$): δ = 21.28 (–$CH(\underline{CH_3})_2$), 28.14 (–$\underline{CH}(CH_3)_2$), 110.68 (C-5′), 122.32 (C-3a), 123.84 (C-8), 124.26 (C-5), 126.14 (C-3″, C-5″), 128.59 (C-4″), 129.01 (C-2″, C-6″), 130.50 (C-6), 132.94 (C-1″), 133.38 (C-7), 134.12 (C-4a), 140.29 (C-8a), 153.25 (C-4′), 158.22 (C-8b), 159.10 (C-3), 160.14 (C-2′), 183.75 (C-4); ESI–MS *m/z*: 372.66 $[M + 1]^+$, 373.64 $[M + 2]^+$, 374.64 $[M + 3]^+$; Anal. Calcd. for $C_{22}H_{17}N_3OS$ (371.11): C, 71.14; H, 4.61; N, 11.31. Found: C, 71.35; H, 4.97; N, 11.60.

1-(4-(4-Chlorophenyl)thiazol-2-yl)-3-isopropylindeno[1,2-c]pyrazol-4(1H)-one (***3j***) Yellow solid; yield 75 %; mp 192–194 °C; IR (KBr): ν_{max} 752, 878, 1094, 1472, 1545, 1603 (C = N), 1701 (C = O), 2880, 2970 (aliphatic C–H stretch), 3098 (aromatic C–H stretch) cm^{-1}; ^1H NMR (400 MHz, $CDCl_3$): δ = 1.41 (d, 6H, *J* = 6.92 Hz,

–CH(C$\underline{H_3}$)$_2$), 3.08–3.11 (m, 1H, –C$\underline{H}$(CH$_3$)$_2$), 7.30–7.47 (5H, m, H-6, H-7, H-5′, H-3″, H-5″), 7.59 (d, 1H, J = 7.16 Hz, H-5), 7.83 (d, 2H, J = 8.44 Hz, H-2″, H-6″), 8.37 (d, 1H, J = 7.36 Hz, H-8); ^{13}C NMR (100 MHz, $CDCl_3$): δ = 21.25 (–CH(C$\underline{H_3}$)$_2$), 28.13 (–C$\underline{H}$(CH$_3$)$_2$), 111.01 (C-5′), 122.41 (C-3a), 123.63 (C-8), 124.34 (C-5), 127.36 (C-2″, C-6″), 129.20 (C-3″, C-5″), 130.58 (C-6), 132.58 (C-1″), 132.87 (C-4″), 133.32 (C-7), 134.43 (C-4a), 140.26 (C-8a), 152.08 (C-4′), 158.21 (C-8b), 159.18 (C-3), 160.38 (C-2′), 183.65 (C-4); ESI–MS *m/z*: 406.66 [M + 1]$^+$, 407.63 [M + 2]$^+$, 408.65 [M + 3]$^+$, 428.23 [M + Na]$^+$; Anal. Calcd. for $C_{22}H_{16}ClN_3OS$ (405.07): C, 65.10; H, 3.97; N, 10.35. Found: C, 65.32; H, 4.25; N, 10.66.

*3-Isopropyl-1-(4-p-tolylthiazol-2-yl)indeno[1,2-c]pyrazol-4 (1H)-one (**3k**)* Green solid; yield 76 %; mp 160–164 °C; IR (KBr): ν_{max} 741, 878, 1095, 1475, 1543, 1605 (C = N), 1711 (C = O), 2872, 2966 (aliphatic C–H stretch), 3067–3117 (aromatic C–H stretch) cm^{-1}; ^{1}H NMR (400 MHz, $CDCl_3$): δ = 1.41 (d, 6H, J = 6.92 Hz, –CH(C$\underline{H_3}$)$_2$), 2.42 (s, 3H, C$\underline{H_3}$), 3.05–3.12 (m, 1H, –C$\underline{H}$(CH$_3$)$_2$), 7.25–7.46 (5H, m, H-6, H-7, H-5′, H-3″, H-5″), 7.57 (d, 1H, J = 7.16 Hz, H-5), 7.79 (d, 2H, J = 8.08 Hz, H-2″, H-6″), 8.45 (d, 1H, J = 7.40 Hz, H-8); ^{13}C NMR (100 MHz, $CDCl_3$): δ = 21.28 (–CH(C$\underline{H_3}$)$_2$), 21.34 (C$\underline{H_3}$), 28.14 (–C$\underline{H}$(CH$_3$)$_2$), 109.87 (C-5′), 122.27 (C-3a), 123.87 (C-8), 124.21 (C-5), 126.05 (C-3″, C-5″), 129.67 (C-2″, C-6″), 130.45 (C-6), 131.43 (C-1″), 132.98 (C-4a), 133.33 (C-7), 138.54 (C-4″), 140.32 (C-8a), 153.34 (C-4′), 158.17(C-8b), 159.04 (C-3), 160.00 (C-2′), 183.73 (C-4); ESI–MS *m/z*: 386.73 [M + 1]$^+$; Anal. Calcd. for $C_{23}H_{19}N_3OS$ (385.12): C, 71.66; H, 4.97; N, 10.90. Found: C, 71.92; H, 4.68; N, 10.59.

*3-Isopropyl-1-(4-(4-methoxyphenyl)thiazol-2-yl)indeno[1,2 -c]pyrazol-4(1H)-one (**3l**)* Green crystals; yield 77 %; mp 188–190 °C; IR (KBr): ν_{max} 746, 876, 1101, 1481, 1541, 1609 (C = N), 1705 (C = O), 2970 (aliphatic C–H stretch), 3087 (aromatic C–H stretch) cm^{-1}; ^{1}H NMR (400 MHz, $CDCl_3$): δ = 1.41 (d, 6H, J = 6.96 Hz, –CH(C$\underline{H_3}$)$_2$), 3.05–3.12 (m, 1H, –C$\underline{H}$(CH$_3$)$_2$), 3.88 (s, 3H, OC$\underline{H_3}$), 7.00 (d, 2H, J = 8.76 Hz, H-3″, H-5″), 7.16 (s, 1H, H-5′), 7.30–7.47 (m, 2H, H-6, H-7), 7.57 (d, 1H, J = 7.20 Hz, H-5), 7.83 (d, 2H, J = 8.76 Hz, H-2″, H-6″), 8.43 (d, 1H, J = 7.40 Hz, H-8); ^{13}C NMR (100 MHz, $CDCl_3$): δ = 21.27 (–CH(C$\underline{H_3}$)$_2$), 28.14 (–C$\underline{H}$(CH$_3$)$_2$), 55.42 (OC$\underline{H_3}$), 108.85 (C-5′), 114.34 (C-3″, C-5″), 122.26 (C-3a), 123.81 (C-8), 124.22 (C-5), 127.03 (C-1″), 127.43 (C-2″, C-6″), 130.44 (C-6), 132.98 (C-4a), 133.31 (C-7), 140.33 (C-8a), 153.06 (C-4′), 158.13 (C-8b), 159.03 (C-3), 159.93 (C-4″), 159.98 (C-2′), 183.71 (C-4); ESI–MS *m/z*: 402.71 [M + 1]$^+$, 403.78 [M + 2]$^+$, 424.71 [M + Na]$^+$; Anal. Calcd. for $C_{23}H_{19}N_3O_2S$ (401.12): C, 68.81; H, 4.77; N, 10.47. Found: C, 68.63; H, 4.98; N, 10.21.

*General procedure for the synthesis of indenopyrazoles (**4**)* A solution of an appropriate indenopyrazole (**3**) (1 mmol), ethylene glycol (15 mL), hydrazine hydrate (1 mL) and KOH (0.5 mL) was refluxed at 197–200 °C for 5 h. Thereafter, the reaction mixture was poured in ice-cold water. The solid thus obtained was filtered, washed with water, dried and recrystallized from chloroform to afford indenopyrazoles (**4a**–**4l**) in moderate-to-good yields. The physical and spectral data of **4a**–**4l** are given as follows:

*2-(3-Isobutylindeno[1,2-c]pyrazol-1(4H)-yl)-4-phenylthiazole (**4a**)* Offwhite solid; yield 65 %; mp 116–120 °C; IR (KBr): ν_{max} 731, 1020, 1080, 1472, 1508, 1537 (C = N), 2870, 2953 (aliphatic C–H stretch), 3055, 3127 (aromatic C–H stretch) cm^{-1}; ^{1}H NMR (400 MHz, $CDCl_3$): δ = 0.98 (d, 6H, J = 6.80 Hz, –CH$_2$CH(C$\underline{H_3}$)$_2$), 2.02–2.08 (m, 1H, –CH$_2$C$\underline{H}$(CH$_3$)$_2$), 2.61 (d, 2H, J = 6.80 Hz, –C$\underline{H_2}$CH(CH$_3$)$_2$), 3.59 (s, 2H, H-4), 7.29–7.54 (m, 6H, H-6, H-7, H-5′, H-3″, H-4″, H-5″), 7.77 (d, 1H, J = 7.20 Hz, H-5), 8.00 (d, 2H, J = 7.20 Hz, H-2″, H-6″), 8.85 (d, 1H, J = 8.00 Hz, H-8); ^{13}C NMR (100 MHz, $CDCl_3$): δ = 22.13 (–CH$_2$CH(C$\underline{H_3}$)$_2$), 27.63 (C-4), 27.84 (–CH$_2$C$\underline{H}$(CH$_3$)$_2$), 36.15 (–C$\underline{H_2}$CH(CH$_3$)$_2$), 110.83 (C-5′), 121.22 (C-8), 125.63 (C-7), 126.17 (C-2″, C-6″), 128.43 (C-4″), 128.76 (C-6), 128.92 (C-3a), 129.04 (C-3″, C-5″), 132.66 (C-1″), 134.78 (C-5), 138.51 (C-8a), 141.39 (C-4a), 148.59 (C-8b), 153.16 (C-4′), 154.37 (C-3), 159.65 (C-2′); ESI–MS *m/z*: 372.3 [M + 1]$^+$; Anal. Calcd. for $C_{23}H_{21}N_3S$ (371.15): C, 74.36; H, 5.70; N, 11.31. Found: C, 74.59; H, 5.93; N, 11.03.

*4-(4-Chlorophenyl)-2-(3-isobutylindeno[1,2-c]pyrazol-1 (4H)-yl)thiazole (**4b**)* Offwhite solid; yield 64 %; mp 126–129 °C; IR (KBr): ν_{max} 737, 1026, 1078, 1479, 1518, 1531 (C = N), 2889, 2932 (aliphatic C–H stretch), 3051, 3117 (aromatic C–H stretch) cm^{-1}; ^{1}H NMR (400 MHz, $CDCl_3$): δ = 0.99 (d, 6H, J = 6.40 Hz, –CH$_2$CH(C$\underline{H_3}$)$_2$), 2.02–2.08 (m, 1H, –CH$_2$C$\underline{H}$(CH$_3$)$_2$), 2.61 (d, 2H, J = 6.80 Hz, –C$\underline{H_2}$CH(CH$_3$)$_2$), 3.59 (s, 2H, H-4), 7.24–7.55 (m, 5H, H-6, H-7, H-5′, H-3″, H-5″), 7.76 (d, 1H, J = 7.20 Hz, H-5), 7.92 (d, 2H, J = 8.40 Hz, H-2″, H-6″), 8.77 (d, 1H, J = 7.60 Hz, H-8); ^{13}C NMR (100 MHz, $CDCl_3$): δ = 22.20 (–CH$_2$CH(C$\underline{H_3}$)$_2$), 27.69 (C-4), 27.81 (–CH$_2$C$\underline{H}$(CH$_3$)$_2$), 36.12 (–C$\underline{H_2}$CH(CH$_3$)$_2$), 111.09 (C-5′), 121.15 (C-8), 124.15 (C-7), 127.52 (C-2″, C-6″), 128.87 (C-3a), 129.25 (C-3″. C-5″), 129.87 (C-6), 132.53 (C-1″), 132.78 (C-4″), 134.60 (C-5), 138.42 (C-8a), 141.33 (C-4a), 148.66 (C-8b), 152.49 (C-4′), 154.37 (C-3), 159.63 (C-2′); ESI–MS *m/z*: 406.0 [M + 1]$^+$, 407.2 [M + 2]$^+$; Anal. Calcd. for $C_{23}H_{20}ClN_3S$ (405.11): C,

68.05; H, 4.97; N, 10.35. Found: C, 68.36; H, 4.71; N, 10.06.

*2-(3-Isobutylindeno[1,2-c]pyrazol-1(4H)-yl)-4-p-tolylthiazole (**4c**)* Offwhite solid; yield 57 %; mp 115–118 °C; IR (KBr): ν_{max} 742, 1020, 1067, 1460, 1529, 1530 (C = N), 2901, 2943 (aliphatic C–H stretch), 3049, 3121 (aromatic C–H stretch) cm^{-1}; ^{1}H NMR (400 MHz, $CDCl_3$): δ = 0.99 (d, 6H, J = 6.40 Hz, –$CH_2CH(C\underline{H}_3)_2$), 2.02–2.09 (m, 1H, –$CH_2C\underline{H}(CH_3)_2$), 2.43 (s, 3H, $C\underline{H}_3$), 2.61 (d, 2H, J = 7.20 Hz, –$C\underline{H}_2CH(CH_3)_2$), 3.59 (s, 2H, H-4), 7.19–7.53 (m, 5H, H-6, H-7, H-5′, H-3″, H-5″), 7.77 (d, 1H, J = 7.20 Hz, H-5), 7.88 (d, 2H, J = 8.40 Hz, H-2″, H-6″), 8.85 (d, 1H, J = 7.60 Hz, H-8); ^{13}C NMR (100 MHz, $CDCl_3$): δ = 21.32 ($\underline{C}H_3$), 22.18 (–$CH_2CH(\underline{C}H_3)_2$), 27.67 (C-4), 27.74 (–$CH_2\underline{C}H(CH_3)_2$), 36.20 (–$\underline{C}H_2CH(CH_3)_2$), 109.99 (C-5′), 121.17 (C-8), 125.35 (C-7), 126.09 (C-2″, C-6″), 128.89 (C-3a), 129.43 (C-6), 129.62 (C-3″, C-5″), 131.49 (C-1″), 134.75 (C-5), 138.34 (C-4″), 138.62 (C-8a), 141.49 (C-4a), 148.41 (C-8b), 153.51 (C-4′), 154.43 (C-3), 159.51 (C-2′); ESI–MS *m/z*: 386.2 $[M + 1]^+$, 387.3 $[M + 2]^+$, 408.2 $[M + Na]^+$; Anal. Calcd. for $C_{24}H_{23}N_3S$ (385.16): C, 74.77; H, 6.01; N, 10.90; S, 8.32. Found: C, 74.46; H, 6.37; N, 10.68; S, 8.56.

*2-(3-Isobutylindeno[1,2-c]pyrazol-1(4H)-yl)-4-(4-methoxyphenyl)thiazole (**4d**)* Offwhite solid; yield 55 %; mp 120–122 °C; IR (KBr): ν_{max} 735, 1036, 1070, 1466, 1514, 1543 (C = N), 2851, 2955 (aliphatic C–H stretch), 3055, 3117 (aromatic C–H stretch) cm^{-1}; ^{1}H NMR (400 MHz, $CDCl_3$): δ = 1.02 (d, 6H, J = 6.80 Hz, –$CH_2CH(C\underline{H}_3)_2$), 2.11–2.18 (m, 1H, –$CH_2C\underline{H}(CH_3)_2$), 2.65 (d, 2H, J = 7.60 Hz, –$C\underline{H}_2CH(CH_3)_2$), 3.62 (s, 2H, H-4), 3.89 (s, 3H, $OC\underline{H}_3$), 7.03 (2H, d, J = 8.80 Hz, H-3″, H-5″), 7.11 (s, 1H, H-5′), 7.32–7.47 (m, 2H, H-6, H-7), 7.53 (d, 1H, J = 7.60 Hz, H-5), 7.92 (d, 2H, J = 8.80 Hz, H-2″, H-6″), 8.83 (d, 1H, J = 7.60 Hz, H-8); ^{13}C NMR (100 MHz, $CDCl_3$): δ = 22.16 (–$CH_2CH(\underline{C}H_3)_2$), 27.71 (C-4), 27.78 (–$CH_2\underline{C}H(CH_3)_2$), 36.15(–$\underline{C}H_2CH(CH_3)_2$), 55.45 ($O\underline{C}H_3$), 108.97 (C-5′), 114.25 (C-3″, C-5″), 121.13 (C-8), 124.38 (C-7), 127.08 (C-2″, C-6″), 127.53 (C-1″), 129.07 (C-3a), 129.72 (C-6), 134.64 (C-5), 138.51 (C-8a), 141.84 (C-4a), 148.56 (C-8b), 153.22 (C-4′), 154.37 (C-3), 159.95 (C-2′), 159.95 (C-4″); ESI–MS *m/z*: 402.0 $[M + 1]^+$; Anal. Calcd. for $C_{24}H_{23}N_3OS$ (401.16): C, 71.79; H, 5.77; N, 10.47. Found: C, 71.98; H, 5.42; N, 10.75.

*4-Phenyl-2-(3-propylindeno[1,2-c]pyrazol-1(4H)-yl)thiazole (**4e**)* Offwhite solid; yield 52 %; mp 96–98 °C; IR (KBr): ν_{max} 731, 1072, 1470, 1510, 1539 (C = N), 2870, 2957 (aliphatic C–H stretch), 3051, 3128 (aromatic C–H stretch) cm^{-1}; ^{1}H NMR (400 MHz, $CDCl_3$): δ = 0.98 (t, 3H, –$CH_2CH_2C\underline{H}_3$), 1.72–1.81 (m, 2H, –$CH_2C\underline{H}_2CH_3$), 2.71 (t, 2H, –$C\underline{H}_2CH_2CH_3$), 3.59 (s, 2H, H-4), 7.24–7.35 (m, 4H, H-6, H-7, H-5′, H-4″), 7.48 (d, 2H, J = 7.40 Hz, H-3″, H-5″), 7.74 (d, 1H, J = 7.44 Hz, H-5), 7.99 (d, 2H, J = 7.40 Hz, H-2″, H-6″), 8.84 (d, 1H, J = 7.48 Hz, H-8); ^{13}C NMR (100 MHz, $CDCl_3$): δ = 13.91 (–$CH_2CH_2\underline{C}H_3$), 21.79 (–$CH_2\underline{C}H_2CH_3$), 27.70 (C-4), 28.54 (–$\underline{C}H_2CH_2CH_3$), 110.81 (C-5′), 121.13 (C-8), 125.58 (C-7), 126.46 (C-2″, C-6″), 128.67 (C-4″), 128.74 (C-6), 128.80 (C-3″, C-5″), 129.01 (C-3a), 132.78 (C-1″), 134.81 (C-5), 138.48 (C-8a), 141.59 (C-4a), 148.62 (C-8b), 153.35 (C-4′), 154.57 (C-3), 159.62 (C-2′); ESI–MS *m/z*: 358.6 $[M + 1]^+$; Anal. Calcd. for $C_{22}H_{19}N_3S$ (357.13): C, 73.92; H, 5.36; N, 11.75. Found: C, 73.65; H, 5.68; N, 11.37.

*4-(4-Chlorophenyl)-2-(3-propylindeno[1,2-c]pyrazol-1(4H)-yl)thiazole (**4f**)* Offwhite solid; yield 54 %; mp 116–118 °C; IR (KBr): ν_{max} 727, 1082, 1472, 1512, 1539 (C = N), 2872, 2957 (aliphatic C–H stretch), 3051, 3128 (aromatic C–H stretch) cm^{-1}; ^{1}H NMR (400 MHz, $CDCl_3$): δ = 0.96 (t, 3H, –$CH_2CH_2C\underline{H}_3$), 1.70–1.80 (m, 2H, –$CH_2C\underline{H}_2CH_3$), 2.72 (t, 2H, –$C\underline{H}_2CH_2CH_3$), 3.58 (s, 2H, H-4), 7.24–7.33 (m, 3H, H-6, H-7, H-5′), 7.47 (d, 2H, J = 8.64 Hz, H-3″, H-5″), 7.73 (d, 1H, J = 7.40 Hz, H-5), 7.90 (d, 2H, J = 8.64 Hz, H-2″, H-6″), 8.77 (d, 1H, J = 7.60 Hz, H-8); ^{13}C NMR (100 MHz, $CDCl_3$): δ = 13.90 (–$CH_2CH_2\underline{C}H_3$), 21.80 (–$CH_2\underline{C}H_2CH_3$), 27.71 (C-4), 28.56 (–$\underline{C}H_2CH_2CH_3$), 111.08 (C-5′), 121.12 (C-8), 124.04 (C-7), 126.79 (C-2″, C-6″), 128.89 (C-3a), 129.27 (C-3″, C-5″), 129.99 (C-6), 132.53 (C-1″), 132.81 (C-4″), 134.87 (C-5), 138.87 (C-8a), 141.23 (C-4a), 148.65 (C-8b), 153.51 (C-4′), 154.31 (C-3), 159.45 (C-2′); ESI–MS *m/z*: 392.1 $[M + 1]^+$. Anal. Calcd. for $C_{22}H_{18}ClN_3S$ (391.09): C, 67.42; H, 4.63; N, 10.72. Found: C, 67.73; H, 4.34; N, 10.46.

*2-(3-Propylindeno[1,2-c]pyrazol-1(4H)-yl)-4-p-tolylthiazole (**4g**)* Offwhite solid; yield 58 %; mp 117–120 °C; IR (KBr): ν_{max} 727, 1082, 1474, 1508, 1543 (C = N), 2872, 2957 (aliphatic C–H stretch), 3053, 3128 (aromatic C–H stretch) cm^{-1}; ^{1}H NMR (400 MHz, $CDCl_3$): δ = 0.95 (t, 3H, –$CH_2CH_2C\underline{H}_3$), 1.69–1.79 (m, 2H, –$CH_2C\underline{H}_2CH_3$), 2.42 (s, 3H, $C\underline{H}_3$), 2.70 (t, 2H, –$C\underline{H}_2CH_2CH_3$), 3.57 (s, 2H, H-4), 7.23–7.34 (m, 3H, H-6, H-7, H-5′), 7.47 (d, 2H, J = 8.24 Hz, H-3″, H-5″), 7.72 (d, 1H, J = 7.28 Hz, H-5), 8.04 (d, 2H, J = 8.24 Hz, H-2″, H-6″), 8.84 (d, 1H, J = 7.40 Hz, H-8); ^{13}C NMR (100 MHz, $CDCl_3$): δ = 13.90 (–$CH_2CH_2\underline{C}H_3$), 21.36 ($\underline{C}H_3$), 21.80 (–$CH_2\underline{C}H_2CH_3$), 27.70 (C-4), 28.55 (–$\underline{C}H_2CH_2CH_3$), 110.02 (C-5′), 121.12 (C-8), 124.61 (C-7), 125.75 (C-2″, C-6″), 129.05 (C-3a), 129.30 (C-3″, C-5″), 129.43 (C-6), 131.41 (C-1″), 134.92 (C-5), 138.57 (C-4″), 138.66 (C-8a), 141.35 (C-4a), 148.69 (C-8b), 153.41 (C-4′), 154.28 (C-3), 159.39 (C-2′); ESI–MS *m/z*: 372.2 $[M + 1]^+$; Anal. Calcd. for $C_{23}H_{21}N_3S$ (371.15): C, 74.36; H, 5.70; N, 11.31. Found: C, 74.58; H, 5.43; N, 11.57.

*4-(4-Methoxyphenyl)-2-(3-propylindeno[1,2-c]pyrazol-1(4H)-yl)thiazole (**4h**)* Offwhite solid; yield 63 %; mp 104–110 °C; IR (KBr): ν_{max} 729, 1078, 1468, 1506, 1537 (C = N), 2875, 2955 (aliphatic C–H stretch), 3049, 3128 (aromatic C–H stretch) cm^{-1}; ^1H NMR (400 MHz, $CDCl_3$): $\delta = 0.98$ (t, 3H, $–CH_2CH_2C\underline{H_3}$), 1.72–1.81 (m, 2H, $–CH_2C\underline{H_2}CH_3$), 2.71 (t, 2H, $–C\underline{H_2}CH_2CH_3$), 3.59 (s, 2H, H-4), 3.88 (s, 3H, OCH_3), 7.17 (d, 2H, J = 8.68 Hz, H-3″, H-5″), 7.24–7.49 (m, 5H, H-6, H-7, H-5′), 7.73 (d, 1H, $J = 7.44$ Hz, H-5), 7.93 (d, 2H, $J = 8.24$ Hz, H-2″, H-6″), 8.84 (d, 1H, $J = 7.40$ Hz, H-8); ^{13}C NMR (100 MHz, $CDCl_3$): $\delta = 13.91$ ($–CH_2CH_2\underline{CH_3}$), 21.80 ($–CH_2\underline{CH_2}CH_3$), 27.71 (C-4), 28.55 ($–\underline{CH_2}CH_2CH_3$), 55.42 ($O\underline{CH_3}$), 109.46 (C-5′), 114.12 (C-3″, C-5″), 121.13 (C-8), 124.07 (C-7), 126.81 (C-2″, C-6″), 126.88 (C-1″), 129.07 (C-3a), 129.72 (C-6), 134.82 (C-5), 138.51 (C-8a), 141.76 (C-4a), 148.63 (C-8b), 153.37 (C-4′), 154.83 (C-3), 159.43 (C-2′), 159.54 (C-4″); ESI–MS *m/z*: 388.1 $[M + 1]^+$; Anal. Calcd. for $C_{23}H_{21}N_3OS$ (387.14): C, 71.29; H, 5.46; N, 10.84. Found: C, 71.45; H, 5.68; N, 10.56.

*2-(3-Isopropylindeno[1,2-c]pyrazol-1(4H)-yl)-4-phenylthiazole (**4i**)* Offwhite solid; yield 66 %; mp 97–101 °C; IR (KBr): ν_{max} 731, 1074, 1466, 1504, 1543 (C = N), 2874, 2961 (aliphatic C–H stretch), 3057, 3211 (aromatic C–H stretch) cm^{-1}; ^1H NMR (400 MHz, $CDCl_3$): $\delta = 1.35$ (d, 6H, $J = 6.96$ Hz, $–CH(C\underline{H_3})_2$), 3.06–3.13 (m, 1H, $–C\underline{H}(CH_3)_2$), 3.62 (s, 2H, H-4), 7.26–7.36 (m, 4H, H-6, H-7, H-5′, H-4″), 7.46 (d, 2H, $J = 7.76$ Hz, H-3″, H-5″,), 7.72 (d, 1H, $J = 7.40$ Hz, H-5), 8.14 (d, 2H, $J = 7.76$ Hz, H-2″, H-6″), 8.70 (d, 1H, $J = 7.60$ Hz, H-8); ^{13}C NMR (100 MHz, $CDCl_3$): $\delta = 21.98$ ($–CH(\underline{CH_3})_2$), 26.28 (C-4), 29.09 ($–\underline{CH}(CH_3)_2$), 110.76 (C-5′), 121.13 (C-8), 125.77 (C-7), 126.40 (C-2″, C-6″), 128.63 (C-4″), 128.76 (C-6), 128.82 (C-3a), 129.08 (C-3″, C-5″), 132.66 (C-1″), 134.78 (C-5), 138.42 (C-8a), 141.39 (C-4a), 148.74 (C-8b), 153.29 (C-4′), 155.24 (C-3), 159.27 (C-2′); ESI–MS *m/z*: 358.21 $[M + 1]^+$; Anal. Calcd. for $C_{22}H_{19}N_3S$ (357.13): C, 73.92; H, 5.36; N, 11.75. Found: C, 73.62; H, 5.71; N, 11.39.

*4-(4-Chlorophenyl)-2-(3-isopropylindeno[1,2-c]pyrazol-1(4H)-yl)thiazole (**4j**)* Offwhite solid; yield 54 %; mp 103–106 °C; IR (KBr): ν_{max} 735, 1082, 1470, 1499, 1536 (C = N), 2910, 2963 (aliphatic C–H stretch), 3057, 3155 (aromatic C–H stretch) cm^{-1}; ^1H NMR (400 MHz, $CDCl_3$): $\delta = 1.37$ (d, 6H, $J = 6.96$ Hz, $–CH(C\underline{H_3})_2$), 3.07–3.14 (m, 1H, $–\underline{CH}(CH_3)_2$), 3.64 (s, 2H, H-4), 7.24–7.34 (m, 3H, H-6, H-7, H-5′), 7.47 (d, 2H, $J = 8.40$ Hz, H-3″, H-5″), 7.74 (d, 1H, $J = 7.36$ Hz, H-5), 7.94 (d, 2H, $J = 8.40$ Hz, H-2″, H-6″), 8.74 (d, 1H, $J = 7.60$ Hz, H-8); ^{13}C NMR (100 MHz, $CDCl_3$): $\delta = 21.92$ ($–CH(\underline{CH_3})_2$), 26.25 (C-4), 29.05 ($–\underline{CH}(CH_3)_2$), 111.22 (C-5′), 121.16 (C-8), 124.49 (C-7), 127.34 (C-2″, C-6″), 128.81 (C-3a), 129.10 (C-3″, C-5″), 129.28 (C-6), 132.16 (C-1″), 132.78 (C-4″), 134.76 (C-5), 138.56 (C-8a), 141.19 (C-4a), 148.67 (C-8b), 152.67 (C-4′), 155.24 (C-3), 159.66 (C-2′); ESI–MS *m/z*: 392.4 $[M + 1]^+$; Anal. Calcd. for $C_{22}H_{18}ClN_3S$ (391.09): C, 67.42; H, 4.63; N, 10.72. Found: C, 67.78; H, 4.32; N, 10.43.

*2-(3-Isopropylindeno[1,2-c]pyrazol-1(4H)-yl)-4-p-tolylthiazole (**4k**)* Offwhite solid; yield 56 %; mp 96–102 °C; IR (KBr): ν_{max} 735, 1071, 1477, 1506, 1545 (C = N), 2874, 2961 (aliphatic C–H stretch), 3059, 3159 (aromatic C–H stretch) cm^{-1}; ^1H NMR (400 MHz, $CDCl_3$): $\delta = 1.37$ (d, 6H, $J = 6.96$ Hz, $–CH(C\underline{H_3})_2$), 2.42 (s, 3H, $C\underline{H_3}$), 3.07–3.14 (m, 1H, $–C\underline{H}(CH_3)_2$), 3.64 (s, 2H, H-4), 7.17–7.48 (m, 5H, H-6, H-7, H-5′, H-3″, H-5″), 7.74 (d, 1H, $J = 7.40$ Hz, H-5), 7.87 (d, 2H, $J = 8.04$ Hz, H-2″, H-6″), 8.86 (d, 1H, $J = 7.60$ Hz, H-8); ^{13}C NMR (100 MHz, $CDCl_3$): $\delta = 21.32$ ($\underline{CH_3}$), 21.92 ($–CH(\underline{CH_3})_2$), 26.24 (C-4), 29.04 ($–\underline{CH}(CH_3)_2$), 108.11 (C-5′), 121.09 (C-8), 125.52 (C-7), 125.76 (C-2″, C-6″), 128.96 (C-3), 129.55 (C-6), 129.63 (C-3″, C-5″), 132.00 (C-1″), 134.75 (C-5), 138.04 (C-4″), 138.65 (C-8a), 141.24 (C-4a), 148.66 (C-8b), 152.75 (C-4′), 155.28 (C-3), 159.64 (C-2′); ESI–MS *m/z*: 372.1 $[M + H]^+$; Anal. Calcd. for $C_{23}H_{21}N_3S$ (371.15): C, 74.36; H, 5.70; N, 11.31. Found: C, 74.65; H, 5.39; N, 11.62.

*2-(3-Isopropylindeno[1,2-c]pyrazol-1(4H)-yl)-4-(4-methoxyphenyl)thiazole (**4l**)* Offwhite solid; yield 51 %; mp 110–114 °C; IR (KBr): ν_{max} 731, 1072, 1474, 1506, 1541 (C = N), 2876, 2961 (aliphatic C–H stretch), 3057, 3157 (aromatic C–H stretch) cm^{-1}; ^1H NMR (400 MHz, $CDCl_3$): $\delta = 1.38$ (d, 6H, $J = 6.92$ Hz, $–CH(C\underline{H_3})_2$), 3.07–3.16 (m, 1H, $–C\underline{H}(CH_3)_2$), 3.64 (s, 2H, H-4), 3.88 (s, 3H, $OC\underline{H_3}$), 7.04–7.48 (m, 5H, H-6, H-7, H-5′, H-3″, H-5″), 7.74 (d, 1H, $J = 7.40$ Hz, H-5), 8.04 (d, 2H, $J = 8.24$ Hz, H-2″, H-6″), 8.84 (d, 1H, $J = 7.64$ Hz, H-8); ^{13}C NMR (100 MHz, $CDCl_3$): $\delta = 21.95$ ($–CH(\underline{CH_3})_2$), 26.23 (C-4), 29.06 ($–\underline{CH}(CH_3)_2$), 55.45 ($O\underline{CH_3}$), 109.91 (C-5′), 114.10 (C-3″, C-5″), 121.13 (C-8), 125.52 (C-7), 127.02 (C-2″, C-6″), 127.39 (C-1″), 128.64 (C-3a), 129.36 (C-6), 134.27 (C-5), 138.45 (C-8a), 141.35 (C-4a), 148.62 (C-8b), 153.52 (C-4′), 155.28 (C-3), 159.88 (C-2′), 159.97 (C-4″); ESI–MS *m/z*: 388.3 $[M + 1]^+$; Anal. Calcd. for $C_{23}H_{21}N_3OS$ (387.14): C, 71.29; H, 5.46; N, 10.84. Found: C, 71.53; H, 5.75; N, 10.48.

In vitro Anticancer Evaluation

Materials

Dulbecco's modified Eagle's medium (DMEM) and 3-(4,5-dimethylthiazol-2-yl)-2,5-diphenyltetrazolium bromide (MTT) were obtained from Sigma Chemical Co. (St. Louis, MO, USA).

Cell culture and treatment

A498 (Human renal carcinoma), HT29 (Human colorectal adenocarcinoma), MCF-7 (Human breast adenocarcinoma), HepG2 (Human hepatocellular carcinoma) and NRK (Normal rat kidney epithelial) cell lines were obtained from National Centre for Cancer Sciences (NCCS), Pune, India, and grown as a monolayer in DMEM supplemented with 10 % FBS (Fetal Bovine Serum), 100 µg/mL streptomycin and 100 units/mL penicillin. Cells were incubated at 37 °C in an atmosphere of 5 % CO_2. For 96-well plates, cells were seeded at approximately 1.5×10^4 cells per well.

MTT assay

The cell viability was assessed by the MTT colorimetric assay (Denizot and Lang, 1986) which is based on the reduction of MTT by the mitochondrial succinate dehydrogenase of intact cells to a purple formazan product. Briefly, cells were incubated in 96-well micro titer plates for 24 h at 37 °C in a 5 % CO_2 incubator. Following the addition of the test compounds, the plates were incubated for an additional 48 h. Control wells contained medium alone. Three replicate wells were used at each point in the experiments. After 24 h incubation, MTT solution (5 mg/mL in phosphate-buffered saline) was added and incubated for another 4 h. The resulting MTT/formazan product was dissolved by 0.1 mL of isopropanol, and the plates were gently shaken to solubilize the formed formazan. The amount of formazan was determined by measuring the absorbance (OD) at 570 nm using a Bio-Rad 550 enzyme-linked immunosorbent assay (ELISA) microplate reader.

Cell survival was calculated as the percentage MTT inhibition as follows:

$$\%\,\text{growth inhibition} = 100 - (\text{mean OD of individual test group}/\text{mean OD of each control group}) \times 100.$$

The values of IC_{50} (concentration of test compound that is needed to reduce the cell survival fraction to 50 %) were calculated and used as a measure of cellular sensitivity to a given treatment.

QSAR studies

Dataset

The data given in the Table 1 was used to carry out this study. The entire dataset of 22 compounds was divided into training set (18 compounds) and test set (04 compounds), and training set was employed to develop QSAR models.

Structure generation

The structures of the molecules were sketched and optimized using Marvin Sketch. The molecules were prepared on the same conformation of basic skeleton indenopyrazole.

Calculation of descriptors

In order to get a QSAR model, compounds were characterized by the molecular descriptors at all times. The molecular descriptors (863 descriptors including one-, two- and three-dimensional descriptors) were calculated with PaDEL Descriptor 2.12 program (Yap, 2011). The different descriptors can portray a molecule from dissimilar aspects, but a little of them may signify the similar meanings with the same or similar values. The invariable or near-constant descriptors and descriptors with value zero for even one molecule were deleted to lessen repetition and errors. If the pairwise correlation of two descriptors was more than 0.75, the one having higher pair correlation with other descriptors was left out from the original matrix of variables to reduce redundant information. The remaining descriptors underwent the consequent variable selection process.

QSAR modeling and validation

Multiple linear regression (MLR) was used for the development of QSAR models, and the stepwise multiple linear regression variable subset selection was applied for variable selection with SPSS software package [SPSS, 1996]. Different parameters were employed to validate the models. The correlation coefficient R was utilized as an assessment of the goodness-of-fit. Further fitting criteria used were R^2_{adj}, R^2–R^2_{adj}, RMSE (Root mean squared error), MAE (Mean average error), s (standard error of estimate) and F (Fischer's value). In order to authenticate model's robustness and predictive power, the cross-validation coefficient Q^2_{LOO} (leave-one-out) was employed where a model is developed by $n - 1$ compounds and the nth compound is predicted. Each compound is iteratively excluded from the set used for model building and predicted sequentially. An indication of the model performance is accomplished from the cross-validation coefficient, which may be defined as

$$Q^2_{LOO} = (1 - \text{PRESS}/\text{TSS})$$

where TSS is the total sum of squares. PRESS (predictive error sum of squares) is the sum of the squared difference between the observed and the predicted values when the compound is held out from the procedure of fitting. The model with high Q^2_{LOO} value is thought to have high predictive ability. This is the only method that uses all the

Table 1 In vitro anticancer activity of thiazole tethered indenopyrazoles (**3a–3l** & **4a–4l**)

Compound	IC_{50} (μM)				NRK[e] cells % cell viability at 500 μM
	A498[a] cells	HT29[b] cells	MCF-7[c] cells	HepG2[d] cells	
3a	378.20	417.98	256.20	324.80	94.53
3b	105.05	188.34	143.90	132.70	97.24
3c	198.62	123.85	302.10	278.30	89.21
3d	177.01	109.31	209.33	197.32	92.54
3e	107.88	123.38	283.21	245.09	96.11
3f	124.18	110.30	377.90	254.03	94.01
3g	63.11	82.21	121.67	78.43	96.93
3h	74.46	89.90	198.45	178.32	98.03
3i	167.88	288.54	308.12	289.43	99.12
3j	230.89	206.67	311.87	276.45	92.76
3k	234.61	212.80	321.05	298.50	93.58
3l	Inactive	Inactive	Inactive	Inactive	97.44
4a	49.74	34.77	32.09	61.12	89.32
4b	62.10	43.09	56.09	34.70	92.73
4c	52.52	69.08	93.08	44.65	98.32
4d	44.31	35.07	48.65	69.06	97.04
4e	50.30	66.03	102.12	75.30	94.23
4f	44.73	39.76	78.04	86.40	91.23
4g	50.57	79.46	87.30	60.20	87.21
4h	46.30	35.10	67.21	54.20	89.01
4i	52.47	77.34	67.80	89.10	90.84
4j	47.22	41.21	50.21	76.20	94.02
4k	97.73	81.02	170.76	104.20	96.94
4l	88.66	67.39	284.12	186.04	95.23
Cisplatin	8.70	23.10	15.20	12.40	–

[a] Human renal carcinoma cell line

[b] Human colorectal adenocarcinoma cell line

[c] Human breast adenocarcinoma cell line

[d] Human hepatocellular carcinoma cell line

[e] Normal rat kidney epithelial cell line

information on hand and is very pertinent mainly in small datasets as is our case.

However, many studies have proved that Q^2_{LOO} is an imperfect measure of a model predictive ability (Baumann and Stiefl, 2004), and although it is necessary at the time of model development, it is still insufficient for a reliable estimate of model predictive power for totally novel compounds. Leave-many-out cross-validation (LMO-CV) is a stronger CV technique where more than one compound is excluded at a time for the validation. LMO is used to counteract the slight over optimism of Q^2_{LOO}. Moreover, it has been established on different datasets that the strongest CV, that can furnish a more realistic indication of the true internal predictivity in small datasets (20–30 compounds), is LMO 30 % (Gramatica 2007). Therefore, we have used LMO with 30 % compounds left at a time.

Further, to ensure the robustness and the statistical importance of this QSAR study, Y-randomization test was also exercised to validate the developed models. In this test, the Y vector is shuffled randomly and the calculation procedure is repeated various times. The resulting models following several repetitions are supposed to have less significant correlation coefficient values than the ones of the original model. If all models attained by the Y-randomization test have comparatively high values for R^2 statistics, then this is because of a chance correlation and suggests that the present modeling technique cannot lead to a satisfactory model using the existing dataset [Long *et al.,* 2013].

In light of Tropsha's criteria, the predictive power of a QSAR model should be evaluated on an external dataset that has not been taken into account during the process of model building. Therefore, the dataset was split into training (18 compounds) and test set (04 compounds) in order to confirm the true predictive power of the developed models (Tropsha, 2010). Q^2_{ext} was used as a criterion for this estimation which was calculated by formula described in literature (Shi *et al.,* 2001).

Results and discussion

Chemistry

The synthetic route for the preparation of thiazole tethered indenopyrazoles (**3** & **4**) is outlined in Scheme 1. The starting 1,3-diketones, i.e, 2-acyl-(1*H*)-indene-1,3(2*H*)-diones (**1**) were prepared by the Claisen condensation of appropriate ketones and diethylphthlate under the influence of sodium methoxide as per literature procedure (Dhawan *et al.,* 1993; Shapiro *et al.,* 1960). The synthesis of twelve new indeno[1,2-*c*]pyrazol-4-ones (**3**) was carried out by a convenient one-pot three-component reaction of 1,3-diketones (**1**), thiosemicarbazide and α-bromoketones (**2**). Initially, a mixture of appropriate 2-acyl-(1*H*)-indene-1,3(2*H*)-dione (**1**) and thiosemicarbazide was refluxed in methanol for 10 min. Thereafter, the reaction mixture was charged with an appropriate phenacyl bromide (**2**) and glacial acetic acid, and subsequently refluxed for 6–7 h to furnish the corresponding thiazole tethered indeno[1,2-*c*]pyrazol-4-ones (**3a–3l**) in high yields. Further, the indeno[1,2-*c*]pyrazol-4-ones (**3a–3l**) were subjected to Wolff-Kishner reduction (Gupta *et al.,* 1979) to afford the corresponding indenopyrazoles (**4a–4l**) in moderate-to-good yields.

The structures of all the newly synthesized thiazole tethered indenopyrazoles (**3** & **4**) were well established by satisfactory IR, NMR (^{1}H and ^{13}C) and mass spectroscopic data. The IR spectra of indenopyrazoles (**3a–3l**), in each case, displayed a strong absorption band in the region at 1701–1713 cm^{-1} due to >C=O stretching. The salient feature of ^{1}H NMR spectra of indenopyrazoles (**3**) is the downfield shifting of C_8–H (δ 8.35–8.48) as compared to other aromatic protons due to anisotropic-diamagnetic effect of lone pair of electrons present on nitrogen and/or sulfur of thiazole moiety (Dhawan *et al.,* 1994). The other aromatic and aliphatic protons appeared in the expected regions. The ^{13}C NMR spectra of indenopyrazoles (**3**), in each case, displayed a signal in the most downfield region at δ 183.65–184.08 which can safely be assigned to the carbonyl carbon (C_4) (Hughes *et al.,* 1977; Patra and Mishra, 1991). The signals appearing in the regions at δ 152.06–159.18, δ 122.26–123.53 and δ 157.70–158.22 were assigned to the carbon atoms C_3, C_{3a} and C_{8b}, respectively, of the pyrazole ring (Singh *et al.,* 1989). The chemical shifts exhibited in the regions at δ 159.89–160.38 ($C_{2'}$), δ 152.08–153.35 ($C_{4'}$) and δ 108.85–111.01 ($C_{5'}$) corroborated the thiazole character of thiazolyl moiety (Thakar *et al.,* 2010). The signals due to the remaining aliphatic and aromatic carbons were obtained in the expected regions. In addition, the compound **3d** was also characterized by 1D DEPT and 2D NMR techniques such as ^{1}H-^{1}H COSY, HSQC and HMBC.

The IR spectra of indenopyrazoles (**4a–4l**), in each case, exhibited a strong absorption band in the region at 1530–1545 cm^{-1} which was presumably attributed due to CN stretching (Pandya and Khan, 2008). Further, the reduction of carbonyl group of indeno[1,2-*c*]pyrazol-4-ones (**3**) by Wolff-Kishner reduction was confirmed by the disappearance of the absorption band due to > C=O stretching in the IR spectra of indenopyrazoles (**4**) as exhibited by indeno[1,2-*c*]pyrazol-4-ones (**3**). Also, the appearance of a singlet in ^{1}H NMR spectra of indenopyrazoles (**4a–4l**), in each case, in the region at δ 3.57–3.64 integrating for two protons due to C_4 protons and the downfield shifting of C_8–H (δ 8.70–8.86) most likely due to increased anisotropic-diamagnetic effect of thiazole moiety, further confirms that the hybridization state of C_4 changes from sp^2 to sp^3 by Wolff-Kishner reduction of **3**. The other aliphatic and aromatic protons appeared in the expected regions. The conversion of indeno[1,2-*c*]pyrazol-4-ones (**3**) into indenopyrazoles (**4**) was further supported by disappearance of the signal due to carbonyl carbon (>C=O) and appearance of signal due to CH_2 of indenopyrazole moiety in the region at δ 26.23–27.71 in the ^{13}C NMR spectra of **4**. The remaining aliphatic and aromatic carbons were observed in the expected regions. Further, the results obtained from mass spectral analysis and analytical data of **3** and **4** were found in accordance with their molecular formulae.

In vitro anticancer evaluation

The newly synthesized thiazole tethered indenopyrazole derivatives (**3a–3l** & **4a–4l**) were evaluated for their in vitro cytotoxicity against A498 (Human renal carcinoma), HT29 (Human colorectal adenocarcinoma), MCF-7 (Human breast adenocarcinoma), HepG2 (Human hepatocellular carcinoma) and NRK (Normal rat kidney epithelial) cell lines by performing the standard MTT assay (Denizot and Lang, 1986). Cisplatin was used as reference drug in the present investigation because it is one of the most potent chemotherapeutic drugs used worldwide for over 40 years and easily available. Cisplatin is not specific against any particular organ and has been successfully employed for treatment of various

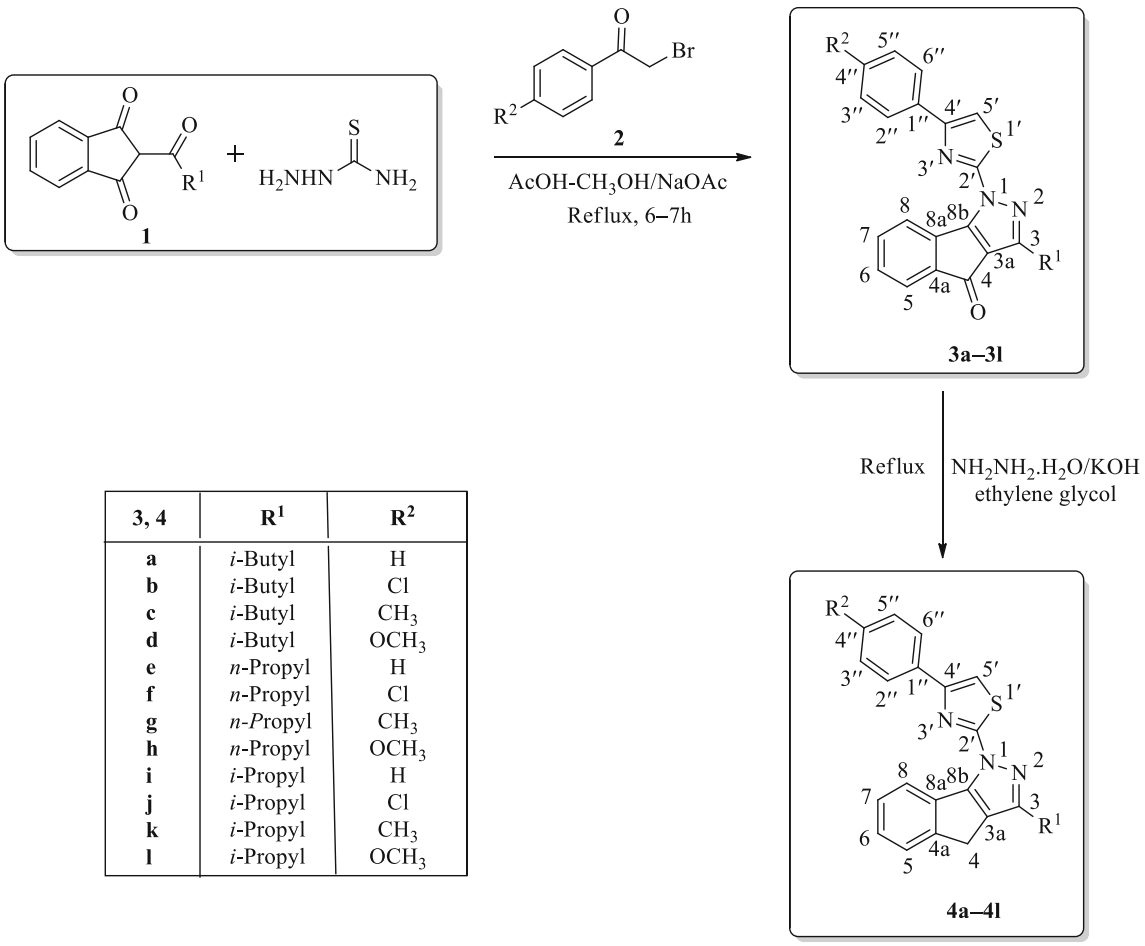

3, 4	R^1	R^2
a	*i*-Butyl	H
b	*i*-Butyl	Cl
c	*i*-Butyl	CH_3
d	*i*-Butyl	OCH_3
e	*n*-Propyl	H
f	*n*-Propyl	Cl
g	*n*-Propyl	CH_3
h	*n*-Propyl	OCH_3
i	*i*-Propyl	H
j	*i*-Propyl	Cl
k	*i*-Propyl	CH_3
l	*i*-Propyl	OCH_3

Scheme 1 Synthetic route of thiazole tethered indenopyrazoles (**3a–3l** & **4a–4l**)

human cancers including bladder, lung, head and neck, ovarian, and testicular cancers. It is effective against many types of cancers including germ cell tumors, carcinomas, sarcomas, lymphomas, and cancers of soft tissue, muscles, bones, and blood vessels. In the present study, cytotoxicity of the synthesized compounds was tested against cell lines of different organs, so a drug specific to a particular organ could not be used as reference molecule.

IC_{50} values of the indenopyrazoles (**3a–3l** & **4a–4l**) against different human cancer cell lines under study are presented in Table 1. It is inferred from the data presented in Table 1 that the indenopyrazoles (**4a–4l**) were found more active than indeno[1,2-*c*]pyrazol-4-ones (**3a–3l**) against all the tested human cancer cell lines. Among all the tested indenopyrazoles, the compound **4d** (IC_{50}, 44.31 μM) was found to be most effective against A498 cancer cell line and the derivatives **4a** (IC_{50}, 34.77 μM), **4d** (IC_{50}, 35.07 μM) and **4h** (IC_{50}, 35.10 μM) exhibited better activity against HT29 cancer cell line. The compound **4a** (IC_{50}, 32.09 μM) showed highest activity against MCF-7 cancer cell line, whereas **4b** (IC_{50}, 34.70 μM) was found more active against HepG2 cancer cell line as compared to other tested derivatives. Further, the results illustrated that compound **3l** was inactive against all the tested human cancer cell lines. It is worth mentioning here that all the tested compounds were found to be less toxic against normal cell line (NRK).

The tested compounds displayed different activities against different cell lines because the selected cell lines belong to different organs of human body. The difference in activities of control cisplatin and tested compounds may be due to their different mechanisms of action. Cisplatin acts by cross-linking DNA in different ways (Kartalou and Essigmann, 2001; Rabik and Dolan, 2007) thereby interfering with cell division by mitosis, which in turn leads to cell cycle arrest and apoptosis. On the other hand, indenopyrazoles are well-known CDK (Nugiel *et al.*, 2002; Usui *et al.*, 2008; Yue *et al.*, 2004) and CHK inhibitors (Tao *et al.*, 2005, 2007).

Quantitative structure–activity relationship (QSAR) studies

In order to understand the observed activity trend on structural basis, QSAR studies were performed for anticancer activities of the synthesized indenopyrazoles (**3a–3l** & **4a–4l**). Anticancer activity data determined as IC_{50} values was first transformed into pIC_{50} values and used as dependent variables in QSAR analysis and is depicted in Table 2. Different 2D and 3D descriptors were calculated for all the active compounds and used as independent variables in this study. The values of descriptors used in successful model development are presented in Table 2. In the present QSAR model development study, a dataset containing twenty-three compounds was used (except compound **3l**) and it was split into training set and a test set excluding outliers. The first step in getting a model with statistical significance is to inspect whether any colinearity exists between the descriptors used. This is accomplished by obtaining correlation matrix (Agrawal *et al.*, 2002). Therefore, correlation matrix displaying correlation between the activity and descriptors as well as intercorrelation among descriptors is displayed in Table 3.

Multiple linear regression analysis was used for creation of QSAR equations. Statistically significant QSAR models were developed, and best split QSAR model developed for A498 cells is expressed by Eq. (1).

QSAR model for anticancer activity against A498 cells

$$\begin{aligned} pIC_{50}\text{A498 cells} = {} & -0.1182(\pm 0.0143)\,\text{MDEC - 33} \\ & + 2.6596(\pm 0.4024) \end{aligned} \quad (1)$$

($n = 18$; $R = 0.900$; $R^2_{adj} = 0.799$; R^2–$R^2_{adj} = 0.012$; $s = 0.112$; $F = 68.590$; RMSE = 0.106; $Q^2_{LOO} = 0.763$; $Q^2_{LMO} = 0.500$, $R^2Y_{scr} = 0.058$; $RMSE_{cv} = 0.202$; $Q^2_{ext} = 0.7134$).

Here and after that, n = number of compounds, R = correlation coefficient, R^2_{adj} = adjusted coefficient of determination, s = standard error, F = Fischer's value, Q^2_{LOO} = cross-validated coefficient (leave one out), Q^2_{LMO} = cross-validated coefficient (leave many out), RMSE = Root Mean Squared Error, $RMSE_{cv}$ = Root Mean Squared Error (cross-validation), $R^2Y_{scr} = R^2$ scrambled, Q^2_{ext} = external cross-validated coefficient.

Statistical data of the model developed reveals that it is a good QSAR model and have high-quality internal predictive

Table 2 pIC_{50} and calculated descriptors of the compounds under study

Comp.		MDEC-33	h_{max}	MDEC-23	maxsCH3	ETA_EtaP_L	Weta2.eneg	pIC_{50} (A498)	pIC_{50} (HT29)	pIC_{50} (MCF-7)	pIC_{50} (HepG2)
3a	Training	14.91434	0.584271	24.10541	2.166221	0.25441	0.490857	0.422278	0.378844	0.591421	0.488384
3b	Training	15.5031	0.5841	25.24228	2.171532	0.25714	0.500167	0.978604	0.725057	0.841939	0.877129
3c	Training	15.5031	0.584271	25.24228	2.168193	0.25852	0.507304	0.701977	0.907104	0.519849	0.555487
3d	Training	15.5031	0.598474	25.24228	2.16054	0.25481	0.495947	0.752002	0.96134	0.679169	0.704829
3e	Test	13.14206	0.584271	24.64319	2.124554	0.25066	0.497564	0.967059	0.908755	0.547891	0.610674
3f	Training	13.60498	0.5841	25.84719	2.129865	0.25362	0.506054	0.905948	0.957424	0.422623	0.595115
3g	Training	13.60498	0.584271	25.84719	2.126527	0.25504	0.40171	1.199902	1.085075	0.914816	1.105518
3h	Training	13.60498	0.596159	25.84719	2.118874	0.25132	0.383785	1.128077	1.04624	0.702349	0.7488
3i	Training	15.81236	0.584271	21.26107	2.094097	0.24683	0.466915	0.775001	0.539794	0.51128	0.538456
3j	Test	16.29097	0.5841	22.30227	2.100283	0.24993	0.463275	0.636595	0.684723	0.506026	0.558383
3k	Training	16.29097	0.584271	22.30227	2.096412	0.25135	0.45286	0.629653	0.672028	0.493427	0.525056
4a	Training	11.49254	0.609554	25.11136	2.272891	0.26777	0.470471	1.303294	1.458795	1.49363	1.213817
4b	Training	12.19495	0.609382	26.37488	2.278202	0.27012	0.480299	1.206908	1.365624	1.251115	1.459671
4c	Training	12.19495	0.609554	26.37488	2.274864	0.27154	0.473819	1.279675	1.160648	1.031144	1.350179
4d	Training	12.19495	0.616498	26.37488	2.267211	0.26725	0.448674	1.353498	1.455064	1.312917	1.160773
4e	Test	9.913058	0.609554	25.2113	2.231225	0.26438	0.460324	1.298432	1.180259	0.990889	1.123205
4f	Training	10.50962	0.609382	26.50701	2.236536	0.26694	0.456444	1.349401	1.400554	1.107683	1.063486
4g	Training	10.50962	0.609554	26.50701	2.233197	0.26842	0.445358	1.296107	1.099851	1.058986	1.220404
4h	Training	10.50962	0.616498	26.50701	2.225544	0.26409	0.424077	1.334419	1.454693	1.172566	1.266001
4i	Training	12.26552	0.609554	22.60752	2.239652	0.26041	0.463982	1.280089	1.111596	1.16877	1.050122
4j	Training	12.87408	0.609382	23.80307	2.245839	0.26312	0.460328	1.325874	1.384997	1.29921	1.118045
4k	Test	12.87408	0.609554	23.80307	2.241967	0.26459	0.450279	1.009972	1.091408	0.767614	0.982132
4l	Training	12.87408	0.616498	23.80307	2.233091	0.2604	0.426526	1.052272	1.171405	0.546498	0.730394

Table 3 Correlation matrix

	MDEC-33	h_{max}	MDEC-23	maxsCH3	ETA_EtaP_L	Weta2.eneg	pIC_{50} (A498)	pIC_{50} (HT29)	pIC_{50} (MCF-7)	pIC_{50} (HepG2)
MDEC-33	1									
h_{max}	−0.79156	1								
MDEC-23	−0.57706	0.358254	1							
maxsCH3	−0.74389	0.882594	0.445862	1						
ETA_EtaP_L	−0.76897	0.823504	0.587428	0.954969	1					
Weta2.eneg	0.30288	−0.3419	−0.09138	−0.02083	−0.05249	1				
pIC_{50} (A498)	−0.85865	0.767405	0.539315	0.711129	0.728952	−0.41482	1			
pIC_{50} (HT29)	−0.79379	0.827477	0.581732	0.765162	0.77195	−0.32838	0.887794	1		
pIC_{50} (MCF-7)	−0.70707	0.72947	0.439409	0.80511	0.79428	−0.20313	0.826052	0.798435	1	
pIC_{50} (HepG2)	−0.77791	0.757264	0.578119	0.818601	0.872953	−0.27416	0.87222	0.809501	0.895419	1

ability with values of $Q^2_{LOO} = 0.543$ and $Q^2_{LMO} = 0.500$. The value of Q^2_{LOO} more than 0.5 is an essential condition for a valid QSAR model (Golbraikh and Tropsha, 2002). Low value of the averaged R^2 scrambled (0.058) was sign of a well-established original model and proved that the model was not obtained by chance. Low values of RMSE prove that the model is free from errors. The high value of Q^2_{ext} (0.7134) verified that the developed model has good external predictive power. The activities predicted by this equation are displayed in Table 4 in conjunction with observed activities and both are matched in the graph shown in Fig. 1. The plot between residuals and observed activities (Fig. 2) demonstrates that the values of residuals are spread on both positive and negative sides of the zero which further verifies that the built model is free from systematic errors. The negative sign of coefficient of MDEC-33 indicate that the activity is correlated with this descriptor in inverse manner. MDEC-33 is molecular distance edge (MDE) 2D parameter describing molecular distance edge between all tertiary carbons (Liu *et al.,* 1998).

MDEC-23 and h_{max} described the anticancer activity of the compounds (**3a–3l** & **4a–4l**) against pHT29 cells, and the best split QSAR model developed is depicted in Eq. (2).

QSAR model for anticancer activity against pHT29 cells

$$\begin{aligned} pIC_{50}\text{HT29 cells} &= 15.497(\pm 5.58)\,\text{hmax} \\ &+ 0.0598(\pm 0.0453)\,\text{MDEC - 23} - 9.7005(\pm 3.1918) \end{aligned} \quad (2)$$

($n = 18$; $R = 0.893$; $R^2_{adj} = 0.770$; R^2–$R^2_{adj} = 0.027$; $s = 0.135$; $F = 29.407$; $Q^2_{LOO} = 0.721$; $Q^2_{LMO} = 0.5875$; $R^2Y_{scr} = 0.1203$; RMSE = 0.123; $RMSE_{cv} = 0.144$; $Q^2_{ext} = 0.920$)

Compound **3a** was found to be outliers in this QSAR model. Positive sign of h_{max} and MDEC-23 established that these descriptors are directly correlated with the activity. The standardized coefficient for h_{max} and MDEC-23 were 0.7243 and 0.3441, respectively. This shows that h_{max} is more contributing toward the activity than MDEC-23. The parameter h_{max} is the maximum hydrogen Estate value for all the atoms in the molecule. It illustrates the hydrogen accessibility of the molecule (Hall and Kier, 1995). MDEC-23 is molecular distance edge (MDE) 2D parameter explaining molecular distance edge between all secondary and tertiary carbons (Liu *et al.,* 1998).

The anticancer activity against MCF-7 cells was described by the subsequent split QSAR Eq. (3).

QSAR model for anticancer activity against MCF-7 cells

$$\begin{aligned} pIC_{50}\text{MCF - 7 cells} &= 4.5459(\pm 1.309)\,\text{maxsCH3} - 9.0565(\pm 2.8741) \end{aligned} \quad (3)$$

($n = 18$; $R = 0.879$; $R^2_{adj} = 0.758$; R^2–$R^2_{adj} = 0.014$; $s = 0.165$; $F = 54.199$; $Q^2_{LOO} = 0.712$; $Q^2_{LMO} = 0.625$; $R^2Y_{scr} = 0.059$; RMSE = 0.155; $RMSE_{cv} = 0.175$; $Q^2_{ext} = 0.566$).

Compound **4l** was found to be outlier; hence, this was left out in model development process. It is a monoparametric model in which descriptor maxsCH3 is correlated with the observed activity in a positive way as the sign of coefficient of this factor is positive. It is an electrotopological state atom type descriptor that explains maximum hydrogen Estate value for all the methyl groups present in the molecule (Hall and Kier, 1995).

Best QSAR model developed for describing anticancer activity against HepG2 cells was biparametric model obtained for 22 compounds (Eq. (4)). Again, compound **4l** was found to be outlier and that is why not used in development of QSAR model.

Table 4 Observed (Obs) and calculated (Cal) activities along with residuals (Res) obtained by the developed QSAR models

Comp.	pIC_{50} (A498)			pIC_{50} (HT29)			pIC_{50} (MCF-7)			pIC_{50} (HepG2)		
	Obs	Cal	Res	Obs	Cal	Res	Obs	Cal	Res	Obs	Cal	Res
3a	–	–	–	–	–	–	0.5914	0.7909	0.1994	0.4884	0.6474	0.159
3b	0.9786	0.8271	−0.1516	0.7251	0.8606	0.1355	0.8419	0.815	−0.0269	0.8771	0.7221	−0.155
3c	0.702	0.8271	0.1251	0.9071	0.8632	−0.0439	0.5198	0.7998	0.28	0.5555	0.7526	0.1971
3d	0.752	0.8271	0.0751	0.9613	1.0833	0.122	0.6792	0.765	0.0859	0.7048	0.6472	−0.0576
3e	0.9671	1.1061	0.1391	0.9088	0.8274	−0.0813	0.5479	0.6014	0.0535	0.6107	0.4866	−0.1241
3f	0.9059	1.0514	0.1455	0.9574	0.8967	−0.0607	0.4226	0.6256	0.203	0.5951	0.5724	−0.0227
3g	1.1999	1.0514	−0.1485	1.0851	0.8994	−0.1857	0.9148	0.6104	−0.3044	1.1055	0.9369	−0.1686
3h	1.1281	1.0514	−0.0766	1.0462	1.0836	0.0374	0.7023	0.5756	−0.1267	0.7488	0.8507	0.1019
3i	0.775	0.7905	0.0155	0.5398	0.6252	0.0854	0.5113	0.463	−0.0483	0.5385	0.4343	−0.1042
3j	0.6366	0.7339	0.0973	0.6847	0.6848	0.0001	0.506	0.4911	−0.0149	0.5584	0.5615	0.0031
3k	0.6297	0.7339	0.1043	0.672	0.6874	0.0154	0.4934	0.4735	−0.0199	0.5251	0.6458	0.1208
4a	1.3033	1.3011	−0.0022	1.4588	1.2472	−0.2116	1.4936	1.2758	−0.2179	1.2138	1.2097	−0.0042
4b	1.2069	1.2181	0.0112	1.3656	1.3201	−0.0455	1.2511	1.2999	0.0488	1.4597	1.2686	−0.1911
4c	1.2797	1.2181	−0.0616	1.1606	1.3228	0.1621	1.0311	1.2847	0.2536	1.3502	1.3412	−0.009
4d	1.3535	1.2181	−0.1354	1.4551	1.4304	−0.0247	1.3129	1.2499	−0.063	1.1608	1.2551	0.0944
4e	1.2984	1.4878	0.1894	1.1803	1.2532	0.0729	0.9909	1.0863	0.0955	1.1232	1.1127	−0.0105
4f	1.3494	1.4173	0.0679	1.4006	1.328	−0.0726	1.1077	1.1105	0.0028	1.0635	1.2203	0.1569
4g	1.2961	1.4173	0.1212	1.0999	1.3307	0.2308	1.059	1.0953	0.0363	1.2204	1.309	0.0886
4h	1.3344	1.4173	0.0829	1.4547	1.4383	−0.0164	1.1726	1.0605	−0.112	1.266	1.2099	−0.0561
4i	1.2801	1.2098	−0.0703	1.1116	1.0975	−0.0141	1.1688	1.1247	−0.0441	1.0501	0.9527	−0.0974
4j	1.3259	1.1378	−0.188	1.385	1.1663	−0.2187	1.2992	1.1528	−0.1464	1.118	1.0654	−0.0527
4k	1.01	1.1378	0.1279	1.0914	1.169	0.0776	0.7676	1.1352	0.3676	0.9821	1.1505	0.1684
4l	1.0523	1.1378	0.0856	1.1714	1.2766	0.1052	–	–	–	–	–	–

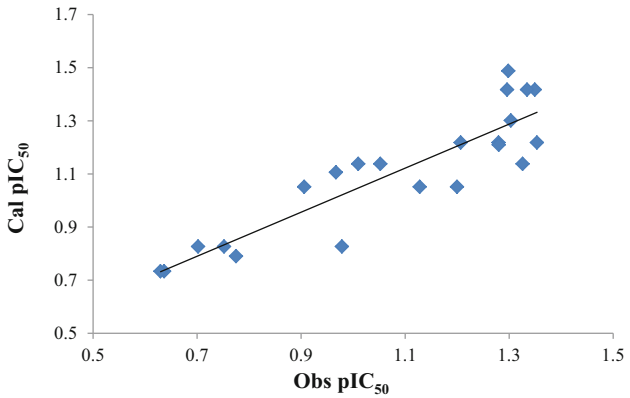

Fig. 1 Plot of observed pIC_{50} against calculated pIC_{50} for the QSAR model of A498 cell lines

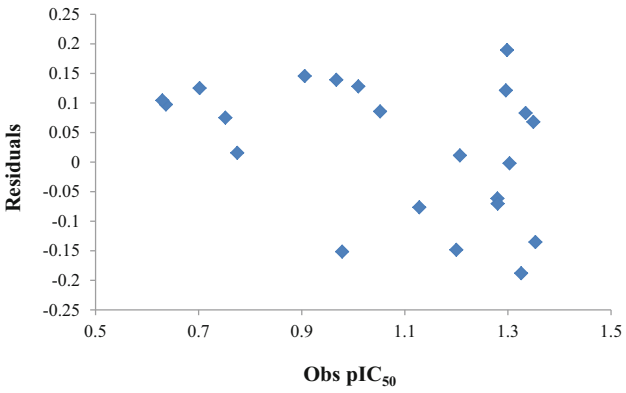

Fig. 2 Plot of observed pIC_{50} against residuals for the QSAR model of A498 cell lines

QSAR model for anticancer activity against HepG2 cells

$$pIC_{50}\text{HepG2 cells} = 37.5356(\pm 8.9206)\,\text{ETA\_EtaP\_L} - 2.9826(\pm 1.9572)\,\text{Weta2.eneg} - 7.438(\pm 2.463) \quad (4)$$

($n = 18$; $R = 0.925$; $R^2_{adj} = 0.837$; $R^2 - R^2_{adj} = 0.019$; $s = 0.129$; $F = 44.550$; $Q^2_{LOO} = 0.783$; $Q^2_{LMO} = 0.751$; $R^2Y_{scr} = 0.121$; $RMSE = 0.118$; $RMSE_{cv} = 0.145$; $Q^2_{ext} = 0.852$).

The coefficient of ETA_EtaP_L is positive illustrating that the activity is related with this descriptor in positive way, whereas Weta2.eneg is correlated in negative manner to the activity, as the coefficient of this parameter is negative in the equation. The standardized coefficients for ETA_EtaP_L and Weta2.eneg are 0.8795 and −0.3185, respectively, establishing more involvement of ETA_EtaP_L in activity determination in contrast to Weta2.eneg. ETA_EtaP_L is an extended topochemical atom descriptor explaining local index extended topochemical atom _local relative to molecular size (Roy and Das, 2011; Roy and Ghosh, 2004). Weta2.eneg is a directional WHIM, weighted by Mulliken atomic electronegativities (Todeschini and Gramatica, 1998).

All the aforementioned models are statistically considerable models as all the statistical parameters are in applicable range. The value of correlation coefficient is more than 0.85 for all the models. In addition, the values of R^2_{adj} are very high and the difference between R^2–R^2_{adj} is very less for all models proving that R^2_{adj} is very close to coefficient of determination of the models. The value of standard error is very small for every model. All these specifics confirm that the developed models have very good fitting capability. The internal predictive ability of all these models is substantiated by high value of leave-one-out cross-validation coefficient (Q^2_{LOO}) as well as leave-many-out cross-validation coefficient (Q^2_{LMO}) which are more than 0.5 and low values of RMSE (Golbraikh and Tropsha, 2002). These facts prove the robustness of the developed models. The difference between RMSE and $RMSE_{cv}$ is very less establishing the fact that described models have sufficient generalizability (Gramatica, 2007).

The developed QSAR models have excellent external predictive power as shown by high values of Q^2_{ext}. The calculated activities, residuals together with observed activities for all above explained QSAR models are presented in Table 4. The plots between observed activity and calculated activity as well as residuals are exhibited in Figs. 3, 4, 5, 6, 7 and 8.

Compound **3a** was outlier for QSAR models 1 and 2, while compound **4l** was outlier for models 3 and 4. These were response outliers for which the reference value of response is invalid as QSAR models developed including these molecules displayed high residual values (Furusjo *et al.,* 2006).

Further, it can be noted that the model no. 2 and 4 which are biparametric models are free from problem of colinearity as the correlation coefficient between the used descriptors is less than 0.4 (Agrawal *et al.,* 2002).

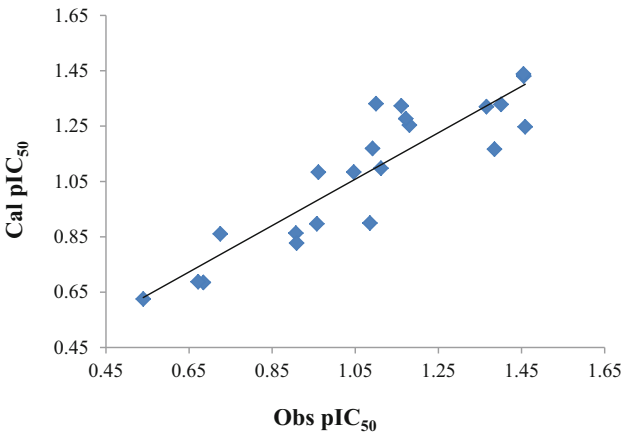

Fig. 3 Plot of observed pIC_{50} against calculated pIC_{50} for the QSAR model of HT29 cell lines

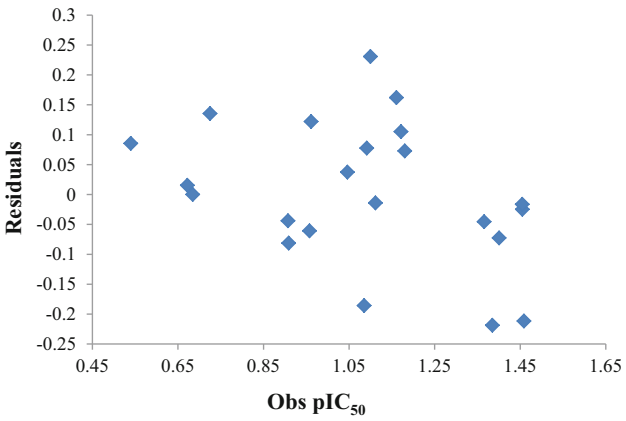

Fig. 4 Plot of observed pIC_{50} against residuals for the QSAR model of HT29 cell lines

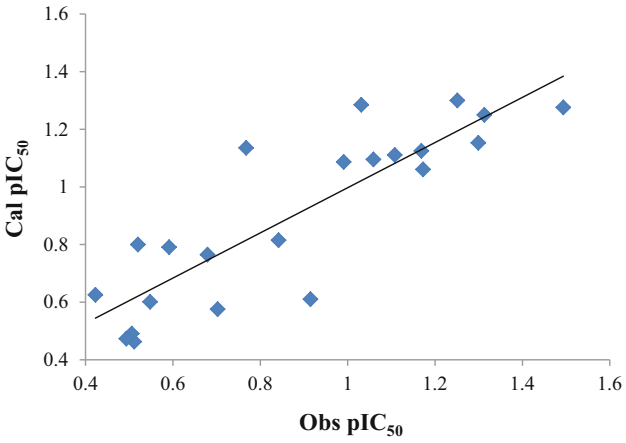

Fig. 5 Plot of observed pIC_{50} against calculated pIC_{50} for the QSAR model of MCF-7 cell lines

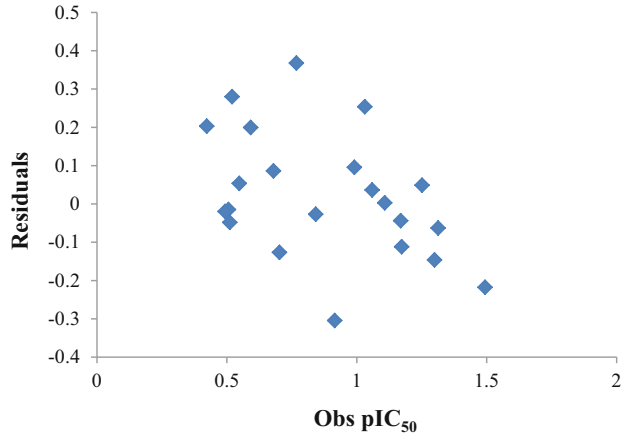

Fig. 6 Plot of observed pIC50 against residuals for the QSAR model of MCF-7 cell lines

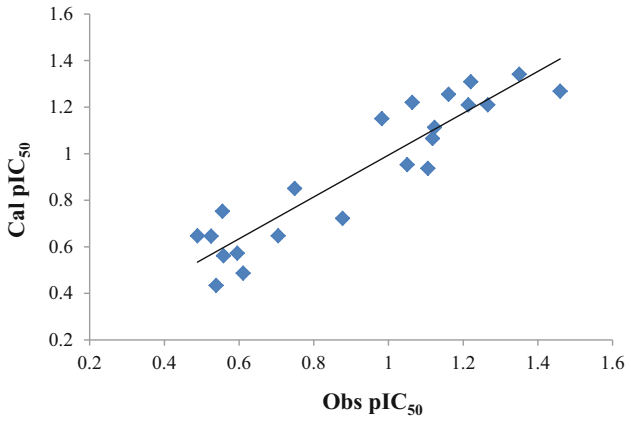

Fig. 7 Plot of observed pIC_{50} against calculated pIC_{50} for the QSAR model of HepG2 cell lines

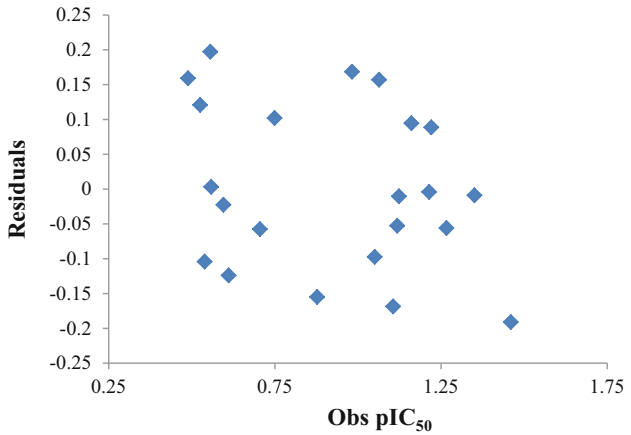

Fig. 8 Plot of observed pIC_{50} against residuals for the QSAR model of HepG2 cell lines

Conclusion

In conclusion, thiazole tethered indeno[1,2-*c*]pyrazol-4-ones (**3**) have been conveniently prepared by three-component one-pot synthesis. Indenopyrazoles (**4**) were synthesized by Wolff-Kishner reduction of **3**. All the newly synthesized thiazole tethered indenopyrazoles (**3** & **4**) are characterized by using different spectral techniques. These indenopyrazoles were evaluated for their in vitro cytotoxicity against A498, HT29, MCF-7, HepG2 and NRK cell lines. Among all the tested indenopyrazoles, **4a**, **4d** and **4h** exhibited better activity against HT29 cancer cell line. Interestingly, all the tested compounds were found to be less toxic toward normal cell line. Further, robust as well as generalizable QSAR models with good fitting ability and internal predictive power were developed for all the cancer cell lines. Molecular distance edge parameters MDEC-33 and MDEC-23 were important for anticancer activity against A498 and HT29 cancer cell lines, respectively, while electrotopological state atom type descriptor maxsCH3 was significant in MCF-7 cell line. Extended topochemical atom descriptor ETA_EtaP_L and directional WHIM parameter Weta2.eneg explained activity trend of HepG2 cell line.

Acknowledgments We gratefully acknowledge the financial support from University Grants Commission, New Delhi, India.

Compliance with ethical standards

Conflict of interest The authors declare that they have no conflict of interest.

References

Abdou MI, Saleh AM, Zohdi HF (2004) Synthesis and antitumor activity of 5-trifluoromethyl-2,4-dihydropyrazol-3-one nucleosides. Molecules 9:109–116

Agrawal VK, Sharma R, Khadikar PV (2002) QSAR studies on antimalarial substituted phenyl analogues and their N^{ω}-Oxides. Bioorg Med Chem 10:1361–1366

Ahsan MJ, Samy JG, Soni S, Jain N, Kumar L, Sharma LK, Yadav H, Saini L, Kalyansing RG, Devenda NS, Prasad R, Jain CB (2011) Discovery of novel antitubercular 3a,4-dihydro-3*H*-indeno[1,2-*c*]pyrazole-2-carboxamide/carbothioamide analogues. Bioorg Med Chem Lett 21:5259–5261

Altıntop MD, Ozdemir A, Ilgın S, Atli O (2014) Synthesis and biological evaluation of new pyrazole-based thiazolyl hydrazone derivatives as potential anticancer agents. Lett Drug Des Discov 11:833–839

Andreani A, Rambaldi M, Mascellani G, Rugarli P (1987) Synthesis and diuretic activity of imidazo[2,1-*b*]thiazole acetohydrazones. Eur J Med Chem 22:19–22

Arshad MF, Siddiqui N, Elkerdasy A, Alrohaimi AH, Khan SA (2014) Anticonvulsant and neurotoxicity evaluation of some

newly synthesized thiazolyl coumarin derivatives. Am J Pharmacol Toxicol 9:132–138

Baumann K, Stiefl N (2004) Validation tools for variable subset regression. J Comput-Aided Mol Des 18:549–562

Bekhit AA, Ashour HMA, Ghany YSA, Bekhit AEA, Baraka A (2008) Synthesis and biological evaluation of some thiazolyl and thiadiazolyl derivatives of 1*H*-pyrazole as anti-inflammatory antimicrobial agents. Eur J Med Chem 43:456–463

Bhosale PP, Chavan RS, Bhosale AV (2012) Design, synthesis, biological evaluation of thiazolyl Schiff base derivatives as novel anti-inflammatory agents. Indian J Chem, Sect B 51:1649–1654

Chong WKM, Duvadie RK (2003) Pyrazole-thiazole compounds, pharmaceutical compositions containing them. US Patent 6566363 B2, Filed Aug 8, 2001, Issued May 20, 2003

Dawood KM, Eldebss TMA, El-Zahabi HAS, Yousef MH, Metz P (2013) Synthesis of some new pyrazole-based 1,3-thiazoles and 1,3,4-thiadiazoles as anticancer agents. Eur J Med Chem 70:740–749

Denizot F, Lang R (1986) Modifications to the tetrazolium dye procedure giving improved sensitivity and reliability. J Immunol Methods 89:271–277

Deverakonda M, Doonaboina R, Vanga S, Vemu J, Boni S, Mailavaram RP (2013) Synthesis of novel 2-alkyl-4-substituted-amino-pyrazolo[3,4-*d*]pyrimidines as new leads for antibacterial and anti-cancer activity. Med Chem Res 22:1090–1101

Dhawan SN, Dasgupta S, Mor S, Gupta SC (1993) Orientational preferences in the synthesis of some indeno[2,1-*c*]quinolin-7(*H*)-ones. Indian J Heterocycl Chem 2:155–158

Dhawan SN, Mor S, Sharma K, Chawla AD, Saini A, Gupta SC (1994) On the mechanism of formation of pyrazoles from 1,3-diketones and hydrazines: isolation of hydroxypyrazoline intermediates. Indian J Chem, Sect B 33:38–42

Elguero J, Goya P, Jagerovic N, Silva AMS (2002) Pyrazoles as drugs: facts and fantasies. In: Attanasi OA, Spinelli D (eds) Targets in heterocyclic systems, vol 6. Royal Society of Chemistry, Cambridge, pp 52–98

Farghaly AA, Bekhit AA, Park JY (2000) Design and synthesis of some oxadiazolyl, thiadiazolyl, thiazolidinyl, and thiazolyl derivatives of 1*H*-pyrazole as anti-inflammatory antimicrobial agents. Arch Pharm Pharm Med Chem 333:53–57

Flores MC, Loev B (1961) Process for preparing pyrazoloindenone hydrazones. US Patent 2,989,538, June 20, 1961

Furusjo E, Svenson A, Rahmberg M, Andersson M (2006) The importance of outlier detection and training set selection for reliable environmental QSAR predictions. Chemosphere 63(1):99–108

Gaikwad ND, Patil SV, Bobade VD (2013) Synthesis and antimicrobial activity of novel thiazole substituted pyrazole derivatives. J Hetrocycl Chem 50:519–527

Golbraikh A, Tropsha A (2002) Beware of q^2! J Mol Graph Model 20:269–276

Gramatica P (2007) Principles of QSAR models validation: internal and external. QSAR Comb Sci 26:694–701

Gu L, Jin C (2012) Synthesis and antitumor activity of α-aminophosphonates containing thiazolo[5,4-*b*]pyridine moiety. Org Biomol Chem 10:7098–7102

Gupta SC, Quarishi MA, Dhawan SN (1979) Synthesis of 6-phenyl-7*H*-indeno[2,1-*c*]quinoline & 2-methyl-6-phenyl-7*H*-indeno[2,1-*c*]quinoline. Indian J Chem, Sect B 18:547–548

Hall LH, Kier LB (1995) Electrotopological state indices for atom types: a novel combination of electronic, topological, and valence state information. J Chem Inf Comput Sci 35:1039–1045

Hamilton RW (1976) The antiarrhythmic and anti-inflammatory activity of a series of tricyclic pyrazoles. J Heterocycl Chem 13:545–553

Hargrave KD, Hess FK, Oliver JT (1983) *N*-(4-substituted thiazolyl)oxamic acid derivatives, new series of potent, orally active antiallergy agents. J Med Chem 26:1158–1163

Hughes DW, Nalliah BC, Holland HL, Maclean DB (1977) ^{13}C nuclear magnetic resonance spectra of the spirobenzylisoquinoline alkaloids and related model compounds. Can J Chem 55:3304–3311

Karale BK, Takate SJ, Salve SP, Zaware BH, Jadhav SS (2015) Synthesis and biological screening of some novel thiazolyl chromones and pyrazoles. Indian J Chem, Sect B 54:798–804

Kartalou M, Essigmann JM (2001) Mechanisms of resistance to cisplatin. Mutation Res 478:23–43

Kim KS, Kimball SD, Misra RN, Rawlins DB, Hunt JT, Xiao HY, Lu S, Qian L, Han WC, Shan W, Mitt T, Cai ZW, Poss MA, Zhu H, Sack JS, Tokarski JS, Chang CY, Pavletich N, Kamath A, Humphreys WG, Marathe P, Bursuker I, Kellar KA, Roongta U, Batorsky R, Mulheron JG, Bol D, Fairchild CR, Lee FY, Webster KR (2002) Discovery of aminothiazole inhibitors of cyclin-dependent kinase 2: synthesis, X-ray crystallographic analysis, and biological activities. J Med Chem 45:3905–3927

Lapenna S, Giordano A (2009) Cell cycle kinases as therapeutic targets for cancer. Nat Rev Drug Discov 8:547–566

Lemke TL, Sawhney KN (1982) The regiospecific synthesis of *N*-substituted pyrazoles. I. 1- and 2-substituted indeno[1,2-*c*]pyrazol-4(1*H*)-ones. J Heterocycl Chem 19:1335–1340

Lemke TL, Cramer MB, Shanmugam K (1978) Heterocyclic tricycles as potential CNS agents I: 4-aminoalkylindeno[1,2-*c*]pyrazoles. J Pharma Sci 67:1377–1381

Lemke TL, Abebe E, Moore PF, Carty TJ (1989) Indeno[1,2-*c*]pyrazolone acetic acids as semirigid analogues of the nonsteroidal anti-inflammatory drugs. J Pharma Sci 78:343–347

Liu S, Cao C, Li Z (1998) Approach to estimation and prediction for normal boiling point (NBP) of alkanes based on a novel molecular distance edge (MDE) Vector, Lambda. J Chem Inf Comput Sci 38:387–394

Loev B, Mosher WA (1961) Pyrazoloindenone azines. US Patent 2,969,374, Jan 24, 1961

Long W, Xiang J, Wu H, Hu W, Zhang X, Jin J, He X, Shen X, Zhou Z, Fan S (2013) QSAR modeling of iNOS inhibitors based on a novel regression method: multi-stage adaptive regression. Chemom Intell Lab Syst 128:83–88

Maggio B, Raffa D, Raidmondi MV, Cusimano MG, Plescia F, Cascioferro S, Cancemi G, Lauricella M, Carlisi D, Daidone G (2014) Synthesis and antiproliferative activity of new derivatives containing the polycyclic system 5,7:7,13-dimethanopyrazolo[3,4-*b*]pyrazolo[3′,4′:2,3]azepino[4,5-*f*]azocine. Eur J Med Chem 72:1–9

Minegishi H, Fukashiro S, Ban HS, Nakamura H (2013) Discovery of indenopyrazoles as a new class of Hypoxia Inducible Factor (HIF)-1 inhibitors. ACS Med Chem Lett 4:297–301

Misra RN, Xiao HY, Kim KS, Lu S, Han WC, Barbosa SA, Hunt JT, Rawlins DB, Shan W, Ahmed SZ, Qian L, Chen BC, Zhao R, Bednarz MS, Kellar KA, Mulheron JG, Batorsky R, Roongta U, Kamath A, Marathe P, Ranadive SA, Sack JS, Tokarski JS, Pavletich NP, Lee FYF, Webster KR, Kimball SD (2004) *N*-(Cycloalkylamino)acyl-2-aminothiazole inhibitors of cyclin-dependent kinase 2. *N*-[5-[[[5-(1,1-Dimethylethyl)-2-oxazolyl]methyl]thio]-2-thiazolyl]-4-piperidinecarboxamide (BMS-387032), a highly efficacious and selective antitumor agent. J Med Chem 47:1719–1728

Mohil R, Kumar D, Mor S (2014) Synthesis and antimicrobial activity of some 1,3-disubstituted indeno[1,2-*c*]pyrazoles. J Heterocycl Chem 51:203–211

Mor S, Mohil R, Kumar D, Ahuja M (2012a) Synthesis and antimicrobial activities of some isoxazolyl thiazolyl pyrazoles. Med Chem Res 21:3541–3548

Mor S, Pahal P, Narasimhan B (2012b) Synthesis, characterization, antimicrobial activities and QSAR studies of some 10a-phenyl-benzo[*b*]indeno[1,2-*e*][1,4]thiazin-11(10a*H*)-ones. Eur J Med Chem 53:176–189

Mor S, Pahal P, Narasimhan B (2012c) Synthesis, characterization, biological evaluation and QSAR studies of 11-p-substituted phenyl-12-phenyl-11*a*,12-dihydro-11*H*-indeno[2,1-*c*][1,5]benzothiazepines as potential antimicrobial agents. Eur J Med Chem 57:196–210

Mosher WA, Soeder RW (1971) 3-Cycloalkyl- and 3-heterocyclic substituted indeno[1,2-*c*]pyrazol-4(1*H*)ones. J Heterocycl Chem 8:855–859

Nugiel DA, Vidwans A, Etzkorn AM, Rossi KA, Benfield PA, Burton CR, Cox S, Doleniak D, Seitz SP (2002) Synthesis and evaluation of indenopyrazoles as cyclin-dependent kinase inhibitors. 2. Probing the indeno ring substituent pattern. J Med Chem 45:5224–5232

Pandya KS, Khan N (2008) Synthesis and antimicrobial study of novel 1-aryl-2-oxo-indano[3,2-*d*]pyrido/pyrimido[1,2-*b*]pyrimidines. Arch Pharm Chem Life Sci 341:418–423

Patra A, Mishra SK (1991) Carbon-13 NMR signals of some substituted indanones, tetralones and benzo-α-pyrones, β-substituted β-phenylpropionic acids and related compounds. Magn Reson Chem 29:749–752

Patt WC, Hamilton HW, Taylor MD, Ryan MJ, Taylor DG Jr, Connolly CJC, Doherty AM, Klutchko SR, Sircar I, Steinbaugh BA, Batley BL, Painchaud CA, Rapundalo ST, Michniewicz BM, Olson SCJ (1992) Structur-activity relationships of a series of 2-amino-4-thiazole containing rennin inhibitors. J Med Chem 35:2562–2572

Penning TD, Talley JJ, Bertenshaw SR, Carter JS, Collins PW, Docter S, Graneto MJ, Lee LF, Malecha JW, Miyashiro JM, Rogers RS, Rogier DJ, Yu SS, Anderson GD, Burton EG, Cogburn JN, Gregory SA, Koboldt CM, Perkins WE, Seibert K, Veenhuizen AW, Zhang YY, Isakson PC (1997) Synthesis and biological evaluation of the 1,5-diarylpyrazole class of cyclooxygenase-2 inhibitors: identification of 4-[5-(4-methylphenyl)-3-(trifluoromethyl)-1*H*-pyrazol-1-yl]benzenesulfonamide (SC-58635, Celecoxib). J Med Chem 40:1347–1365

Pignatello R, Mazzone S, Panico AM, Mazzone G, Penissi G, Castana R, Matera M, Blandino G (1991) Synthesis and biological evaluation of thiazolo-triazole derivatives. Eur J Med Chem 26:929–938

Rabik CA, Dolan ME (2007) Molecular mechanisms of resistance and toxicity associated with platinating agents. Cancer Treatment Rev 33:9–23

Rawal RK, Tripathi R, Katti SB, Pannecouque C, Clercq ED (2008) Design and synthesis of 2-(2,6-dibromophenyl)-3-heteroaryl-1,3-thiazolin-4-ones as anti-HIV agents. Eur J Med Chem 43:2800–2806

Rostom SAF (2006) Synthesis and in vitro antitumor evaluation of some indeno[1,2-*c*]-pyrazol(in)es substituted with sulfonamide, sulfonylurea(-thiourea) pharmacophores, and some derived thiazole ring systems. Bioorg Med Chem 14:6475–6485

Roy K, Das RN (2011) On some novel extended topochemical atom (ETA) parameters for effective encoding of chemical information and modeling of fundamental physicochemical properties. SAR QSAR Environ Res 22:451–472

Roy K, Ghosh G (2004) QSTR with extended topochemical atom indices. 2. Fish toxicity of substituted benzenes. J Chem Inf Comput Sci 44:559–567

Samadhiya P, Sharma R, Srivastava SK (2013) Synthesis and antitubercular activity of 4-oxo-thiazolidine derivatives of 2-amino-5-nitrothiazole. Bull Chem Soc Ethiop 27:249–263

Shapiro L, Geiger K, Freedman L (1960) Indandione anticoagulants. J Org Chem 25:1860–1865

Shi LM, Fang H, Tong W, Wu J, Perkins R, Blair RM, Branham WS, Dial SL, Moland CL, Sheehan DM (2001) QSAR models using a large diverse set of estrogens. J Chem Inf Comput Sci 41:186–195

Shih MH, Su YS, Wu CL (2007) Syntheses of aromatic substituted hydrazine-thiazole derivatives to clarify structural characterization and antioxidant activity between 3-arylsydnonyl and aryl substituted hydrazine-thiazoles. Chem Pharm Bull 55:1126–1135

Sigroha S, Narasimhan B, Kumar P, Khatkar A, Ramasamy K, Mani V, Mishra RK, Majeed ABA (2012) Design, synthesis, antimicrobial, anticancer evaluation and QSAR studies of 4-(substituted benzylidene-amino)-1,5-dimethyl-2-phenyl-1,2-dihydropyrazol-3-ones. Med Chem Res 21:3863–3875

Singh SP, Sehgal S, Tarar LS (1989) Synthesis & NMR spectra of 2-(pyrazol-1yl)benzothiazoles: unambiguous assignment of 3- & 5-substituents of pyrazole moiety. Indian J Chem B 28:27–31

Song YL, Yang T, Dong YF, Wu F, Yang GL (2014) Facile one-pot synthesis of some thiazolyl-pyrazole derivatives with antifungal activity. Chem Lett 43:134–136

Suresh N (2013) Human androgen receptor inhibitors: computational 3D QSAR studies to design lead compounds for treatment of prostate cancer. Turk J Biochem 38:262–269

Tao Z, Sowin TJ, Lin N (2005) A facile synthesis of antitumoral indeno[1,2-*c*]pyrazole-4-one by mild oxidation with molecular oxygen. Tetrahedron Lett 46:7615–7618

Tao Z, Li G, Tong Y, Stewart KD, Chen Z, Bui M, Merta P, Park C, Kover P, Zhang H, Sham HL, Rosenberg SH, Sowin TJ, Lin N (2007) Discovery of 4′-(1,4-dihydro-indeno[1,2-*c*]pyrazol-3-yl)-benzonitriles and 4′-(1,4-diydro-indeno[1,2-*c*]pyrazol-3-yl)-pyridine-2′-carbonitriles as potent checkpoint kinase 1 (Chk1) inhibitors. Bioorg Med Chem Lett 17:5944–5951

Terrett NK, Bell AS, Brown D, Ellis P (1996) (VIAGRA™), a potent and selective inhibitor of type 5cGMP phosphodiesterase with utility for the treatment of male erectile dysfunction. Bioorg Med Chem Lett 6:1819–1824

Thakar AS, Singh KK, Joshi KT, Pancholi AM, Pandya KS (2010) Synthesis, characterization and antibacterial activity of Schiff bases and their metal complexes derived from 4-acyl-1-phenyl-3-methyl-2-pyrazolin-5-ones and 2-amino-4(4′-methylphenyl)-thiazole. E-J Chem 7:1396–1406

Thore SN, Gupta SV, Bhahetui KG (2013) Synthesis and pharmacological investigation of novel substituted thiazole derivatives as non-carboxylic, anti-inflammatory and analgesic agents. Med Chem Res 23:3802–3811

Todeschini R, Gramatica P (1998) New 3D molecular descriptors: the WHIM theory and QSAR applications. Perspect Drug Discov Des 9–11:355–380

Tong J, Zhao X, Zhong L (2014) QSAR studies of imidazo[4,5-*b*]pyridine derivatives as anticancer drugs using RASMS method. Med Chem Res 23:4883–4892

Tropsha A (2010) Best practices for QSAR model development, validation, and exploitation. Mol Inform 29:476–488

Usui T, Ban HS, Kawada J, Hirokawa T, Nakamura H (2008) Discovery of indenopyrazoles as EGFR and VEGFR-2 tyrosine kinase inhibitors by in silico high-throughput screening. Bioorg Med Chem Lett 18:285–288

Wang HH, Qiu KM, Cui HE, Yang YS, Yin-Luo Xing M, Qiu XY, Bai LF, Zhu HL (2013) Synthesis, molecular docking and evaluation of thiazolyl-pyrazoline derivatives containing benzodioxole as potential anticancer agents. Bioorg Med Chem 21:448–455

Yan Z, Caldwell GW, Gauthier D, Leo GC, Mei J, Ho CY, Jones WJ, Masucci JA, Tuman RW, Galemmo RA, Johnson DL (2006) N-Glucuronidation of the platelet-derived growth factor receptor tyrosine kinase inhibitor 6,7-(dimethoxy-2,4-dihydroindeno[1,2-

c]pyrazol-3-yl)-(3-fluoro-phenyl)-amine by human UDP-Glucuronosyltransferases. Drug Metab Dispos 34:748–755

Yap CW (2011) An open source software to calculate molecular descriptors and fingerprints. J Comput Chem 32:1466–1474

Yue EW, DiMeo SV, Higley CA, Markwalder JA, Burton CR, Benfield PA, Grafstrom RH, Cox S, Muckelbauer JK, Smallwood AM, Chen H, Chang C, Trainor GL, Seitz SP (2004) Synthesis and evaluation of indenopyrazoles as cyclin-dependent kinase inhibitors. Part 4: heterocycles at C3. Bioorg Med Chem Lett 14:343–346